Astron. Astrophys. 333, 231–250 (1998)

ASTRONOMY AND ASTROPHYSICS

Model atmospheres broad-band colors, bolometric corrections and temperature calibrations for O - M stars⋆

M.S. Bessell[1], **F. Castelli**[2], **and B. Plez**[3,4]

[1] Mount Stromlo and Siding Spring Observatories, Institute of Advanced Studies, The Australian National University, Weston Creek P.O., ACT 2611, Australia
[2] CNR-Gruppo Nazionale Astronomia and Osservatorio Astronomico di Trieste, Via G.B. Tiepolo 11, I-34131 Trieste, Italy
[3] Astronomiska Observatoriet, Box 515, S-75120 Uppsala, Sweden
[4] Atomspektroskopi, Fysiska Institution, Box 118, S-22100 Lund, Sweden

Received 29 September 1997 / Accepted 3 December 1997

Abstract. Broad band colors and bolometric corrections in the Johnson-Cousins-Glass system (Bessell, 1990; Bessell & Brett, 1988) have been computed from synthetic spectra from new model atmospheres of Kurucz (1995a), Castelli (1997), Plez, Brett & Nordlund (1992), Plez (1995-97), and Brett (1995a,b). These atmospheres are representative of larger grids that are currently being completed. We discuss differences between the different grids and compare theoretical color-temperature relations and the fundamental color temperature relations derived from: (a) the infrared-flux method (IRFM) for A-K stars (Blackwell & Lynas-Gray 1994; Alonso et al. 1996) and M dwarfs (Tsuji et al. 1996a); (b) lunar occultations (Ridgway et al. 1980) and (c) Michelson interferometry (Di Benedetto & Rabbia 1987; Dyck et al. 1996; Perrin et al. 1997) for K-M giants, and (d) eclipsing binaries for M dwarfs. We also compare color - color relations and color - bolometric correction relations and find good agreement except for a few colors. The more realistic fluxes and spectra of the new model grids should enable accurate population synthesis models to be derived and permit the ready calibration of non-standard photometric passbands. As well, the theoretical bolometric corrections and temperature - color relations will permit reliable transformation from observed color magnitude diagrams to theoretical HR diagrams.

Key words: stars: atmospheres; fundamental parameters; general

1. Introduction

The luminosities and temperatures of stars are most often deduced from observed broad-band colors and magnitudes. Empirical color-temperature relations and color - bolometric magnitude corrections are normally used to transform from observed standard magnitudes and colors to temperature and luminosity (eg. bolometric corrections: Schmidt-Kaler 1982; Reid & Gilmore 1984; Bessell & Wood 1984; Tinney et al. 1993; temperatures: Bessell 1979, 1995; Ridgway et al. 1980; Di Benedetto & Rabbia 1987; Blackwell & Lynas-Gray 1994 (BLG94); Tsuji et al. 1995, 1996a; Alonso et al. 1996 (AAM96); Dyck et al. 1996; Perrin et al. 1997). However, apart from AAM96 who give $T_{\rm eff}$ - color relations for F0-K5 dwarfs with both solar and lower than solar metallicity, these empirical data are mostly defined by a restricted group of stars, namely nearby solar composition giants and dwarfs. It is therefore very important to have theoretically derived colors from model atmospheres that can cover the complete range of parameter space, temperature, gravity, composition etc. The empirical data can be compared with the near-solar composition synthetic data to check the goodness of the synthetic data for a restricted set of temperatures, gravities and compositions and by implication the viability of the full theoretical data set.

Model atmosphere grids by Gustafsson et al. (1975) (MARCS) and Kurucz (1979) (ATLAS) have been used successfully by many people over the past 20 years. In particular, discussion of MARCS synthetic photometry was given by Gustafsson & Bell (1979), and Bell & Gustafsson (1989) and of ATLAS synthetic photometry by Buser & Kurucz (1978); however, their limitations due to inadequate lists of atomic and molecular lines and treatment of semi-convection at the intermediate temperatures became more and more evident. Consequently new and improved model atmospheres have been computed making use of the greatly increased computing power and the explosion of data available on atomic and molecular lines from theoretical and experimental work. Kurucz (1993,1994) (ATLAS9) published a new grid of models and colors for O-K stars; the convective models of these grids were later revised by Kurucz (1995a). In addition, some subgrids for convective ATLAS9 models with still a different convection than that used by Kurucz (1995a) were computed by Castelli (1997). Work is in progress to complete them. A new grid by Plez et al. (1997) (NMARCS) for A-M stars is also currently being completed.

We have preliminary published and unpublished data associated with these new grids and they form the basis of this

Send offprint requests to: F. Castelli

⋆ Tables 1-6 are only available in electronic form at the CDS via anonymous ftp to cdsarc.u-strasbg.fr (130.79.128.5) or via http://cdsweb.u-strasbg.fr/Abstract.html

paper. The fluxes, synthetic colors and bolometric corrections are a great improvement over the older data and deserve to be more widely available for use. They suggest that the new grids when completed should enable excellent population synthesis models to be computed from synthetic spectra and colors. They also suggest that non-standard photometric passbands, such as those from the WFPC2 on HST, Hipparcos and MACHO, can be accurately calibrated from synthetic spectra.

The UBVRIJHKL colors presented here have been computed using the passbands defined by Bessell (1990) for the Johnson-Cousins UBVRI photometry and by Bessell & Brett (1988) for the Johnson-Glass JHKL photometry.

In an extensive Appendix we discuss details associated with computing the synthetic photometry, i.e. theoretical magnitudes and colors, and describe how the zeropoints of the standard system and the bolometric corrections were adopted.

In Appendices A and B we describe how the UBVRIJHKL colors were normalised using observed and computed colors for Vega and Sirius.

The bolometric correction BC_X is defined as $m_{bol} = m_X + BC_X$, where X stands for the particular passband. In Appendices C and D, the BC_V bolometric correction zeropoint was derived by *assuming* for the Sun M_{bol} = 4.74 and M_V = 4.81 from the observed V=-26.76 mag (Stebbins & Kron, 1957). Thus we assigned a visual bolometric correction (BC_V) of -0.07 mag for the solar model. *Note that this zeropoint is different to that of -0.193 mag adopted by Kurucz (1979; 1993; 1994) and followed by Schmidt-Kaler (1982)* .

In Appendix E the theoretical realisations of standard system passbands in general and of the UBVRI system in particular are discussed and on the basis of this discussion we decided to scale the raw computed U-B colors by 0.96 as described. The scaled U-B colors are presented in this paper. The other colors have not been adjusted, but it is suggested that they could be adjusted to fit the colors of the hottest and coolest stars, as the standard systems probably incorporate non-linear color terms.

In Appendix F the variation of the effective wavelengths of the UBVRI bands with effective temperature are discussed and theoretical interstellar reddening relations are derived.

2. ATLAS9 and NMARCS model atmospheres

2.1. The ATLAS9 models

Kurucz (1993,1994) has made available models, fluxes, hydrogen line profiles, and colors for a large grid of temperatures, gravities, and abundances. The passbands and zeropoints used by Kurucz were slightly different to those used here, in particular for the Cousins R and I passbands.

Wood & Bessell (1994) computed colors on the UBVRIJHKL system for the Kurucz (1993) fluxes and these have been available via anonymous ftp as ubvrijhkl.dat.z from mso.anu.edu.au at /pub/bessell/. The isochrones of Bertelli et al. (1994) used these synthetic colors and bolometric corrections. These colors were normalised to the standard UBVRIJHKL system in a slightly different way to that described in Appendix A sect. 2. The colors in the present paper essentially supersede those of Wood & Bessell (1994).

In the 1993 flux data there was evidence of some discontinuities in the computed colors of A-G stars. Castelli (1996) explained how to eliminate these discontinuities which were related to a modification of the mixing-length convection adopted by Kurucz for computing the 1993 and 1994 models and called by him "approximate overshooting". The convective models before 1995 were recomputed by Kurucz by adopting the improvement suggested by Castelli for the "approximate overshooting". In Table 1 are presented the colors from the Kurucz 1995 grid of models computed for solar abundance, a microturbulent velocity of 2 km $s^{-1}$and a mixing length to the pressure scale height ratio l/H = 1.25. Because models with $T_{\rm eff} > 8750$K were always computed without any convection, only models with $T_{\rm eff} \leq 8750$K may be different.

Table 2 lists the colors and bolometric corrections for the same set of models as in Table 1 but computed by Castelli with "no-overshoot". Castelli, Gratton & Kurucz (1997) discussed the differences yielded by the overshoot and no overshoot models on some color indices and on Balmer profiles. They showed that the overshoot solar model fits the solar spectra better than the no-overshoot solar model, but that the no-overshoot models should be preferred mostly for stars hotter than the sun.

For completion, Table 3 lists the colors and bolometric corrections for the Kurucz (1994) solar abundance models between 8750K and 50000K and computed for v_{turb}=2 km s^{-1}.

Castelli also computed no-overshoot models for lower metal abundances of -0.5, -1.0, -1.5, -2.0, -2.5 dex and work to extend these grids to more metallicities and microturbulent velocities is in progress. Both the revised 1995 Kurucz grids and the Castelli grids will be distributed on a forthcoming CD-ROM (Kurucz & Castelli, in preparation). In the meantime, the last computed ATLAS9 models and fluxes are available either from kurucz@cfaku3.harvard.edu or from castelli@astrts.oat.ts.astro.it.

2.2. The NMARCS models

The new revised MARCS program incorporating much improved line opacities in the opacity sampling scheme, spherical symmetry and a large number of species in the chemical equilibrium, has been used by Plez, Brett & Nordlund (1992) to model M giants and dwarfs. It has been traditionally divided into SOSMARCS - its spherical version and POSMARCS - the plane-parallel counterpart. There is no reason to separate these two cases for the present purpose and we will adopt NMARCS as a generic name. Initially, Plez, Brett & Nordlund (1992) and Plez (1992) presented a grid of solar composition models. Most of these models were computed for three values of atmospheric extension corresponding to 3 different masses: 1, 2 and 5 $M_\odot$. The higher the mass the less extended are the atmospheres. Another grid was calculated by Plez (1995). It contains mainly hotter, plane-parallel models for a range of scaled solar abundances $[Z/Z_\odot]$ = 0.6, 0.3, 0.0, -0.3, -0.6. These models are available from plez@astro.uu.se. Some improvements were brought to the opacities between these 2 sets, mainly new measurements

of some TiO band strengths by Doverstål & Weijnitz (1992) that replaced some of the earlier values. The 1995 grid was computed at this stage. Subsequently, Hedgecock et al. (1995) performed higher accuracy lifetime measurements for a number of electronic states. These are significantly different from older ones. Langhoff (1997) performed ab initio calculations in good agreement with the latter measurements, and provides electronic transition momenta for all transitions that were included in the present model spectra. The TiO a-f band, affecting the V magnitude, was also added recently. Karlsson et al. (1997) greatly improved the situation for VO by providing lifetime measurements for all 3 excited states A, B, and C. Finally, Jørgensen (1996) provided a line list for H_2O. Alvarez & Plez (1997) used the same data to compute narrow-band colors for M giants and miras and thoroughly discuss these improvements. We decided to recompute the colors of the models using these improved opacities, without, however, reconverging the models structures. Experiments with a few models show that differences in thermal structures are unimportant for the present work. Moreover further improvements in opacities will probably result in changes in both thermal structure and spectra. The next Plez et al. (1997) grid will provide models and spectra from a consistent data set. We found it therefore unnecessary to recompute the whole set of models at the present stage. An indication of the uncertainties/inconsistencies in the model structures is provided by a comparison of the new colors computed for models with identical parameters in the 1992 and 1995 grids (using the $5M_{\odot}$ models in the 1992 grid). At 4000K, log g = 1.5, the difference (1992-1995) in V-K amounts to 0.000, while it is -0.044 at 3800K; at 3600K, log g = 0.0 it is 0.027 and at 4000K, 0.076. In V-I the corresponding differences are 0.000, -0.025, 0.038 and 0.039.

The differences with the older colors (Plez et al. 1992) are small or nonexistent around 4000K and increase with decreasing T_{eff}, esp. for V-I and V-K. We find better agreement with observations using the present improved colors (esp. V-I and BC_I).

Tables 4 and 5 list the colors and bolometric corrections for the Plez et al. (1992) and Plez (1995) models for giants using the newer set of opacities. Brett (1995a,b) computed NMARCS models for M dwarfs which are available from brett@SSMD.MRL.dsto.gov.au. Plez (1997) recomputed a few models with the new NMARCS opacity setup containing the improved opacities. These new models have solar composition, log g = 4.5 (one model for log g=5.5) and temperatures of 3800, 3200, 3000, 2800, 2600, 2400, 2200, and 2000K. Table 6 gives older colors for these Brett M dwarf models together with the improved solar composition dwarf model colors of Plez (1997).

3. Discussion

3.1. Empirical temperature calibrations

Fundamental temperatures are not known for many stars. Radii were measured for some O-F stars by the stellar-intensity interferometer and an empirical temperature scale for early type stars was derived by Code et al. (1976).

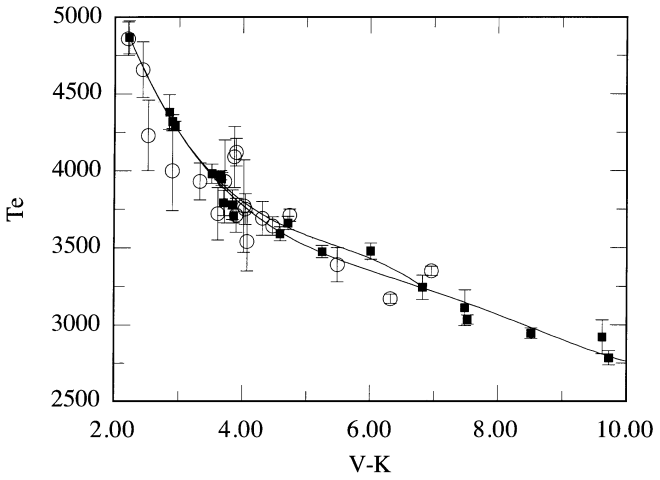

Fig. 1. The empirical $T_{\rm eff}$ versus V-K diagram for giants for the best occultation data of Ridgway et al. (1980) (open circles) and the Michelson interferometer data of Di Benedetto & Rabbia (1987), Dyck et al. (1996) and Perrin et al. (1997) (closed squares). Error bars in the measured temperatures are shown

For cooler giant stars, radii have been derived by lunar occultation and Michelson interferometry. The very influential paper by Ridgway et al. (1980) used lunar occultation data to determine a $T_{\rm eff}$ versus (V-K) relation for KM giants. More recently, Michelson interferometry has been producing much more precise radii for the KM stars and longer baseline interferometers nearing completion will produce very precise radii for hotter stars and for variable stars such as cepheids. Fig. 1 shows the best Ridgway et al. (1980) occultation data and the Di Benedetto & Rabbia (1987), Dyck et al. (1996), and Perrin et al. (1997) interferometer data. There is good agreement between these data although the Michelson derived data has much higher accuracy. The shorter line is the 1980 Ridgway et al. temperature scale. The longer line is a polynomial fit to the interferometer data alone and suggests that a small adjustment only is required to the Ridgway et al. temperature scale between 3700 and 3300K.

For M dwarfs, the empirical data is very scarce there being only two radii measurements, both from eclipsing binary stars. These will be discussed later.

More recently the infrared flux method (IRFM) has been used to derive accurate temperatures for A-M stars. Megessier (1994, 1995) discusses the reliability and accuracy of this technique. Tsuji was amongst the first to promote the IRFM for deriving the temperatures of carbon (Tsuji 1981a) and M giants (Tsuji 1981b) and M dwarfs (Tsuji et al. 1995, 1996a), while Blackwell and co-workers have done much of the pioneering work on hotter stars. BLG94 have derived an effective temperature scale for Pop I A-K giants and dwarfs using the IRFM and the Kurucz (1992) model atmospheres. AAM96 have more recently derived IRFM temperatures and bolometric corrections for F0-K5 dwarfs with a range of metal abundances.

Many authors give their data in terms of V-K which is well suited for K and M giants but is less useful for A and F stars where the lower precision of much V-K photometry (from inde-

pendent measurements of V and K magnitudes) produces larger uncertainties in the $T_{\rm eff}$ -color relations. The color V-I is the more useful temperature sensitive color for A-K stars but unfortunately is not available for all the calibrating stars. However, precise b-y values are available for many stars, particularly the brighter ones and b-y can be converted into V-I very accurately for Pop I A-G stars. We have therefore obtained b-y from Hauck & Mermilliod (1990) for almost all the BLG94, AAM96 and Code et al. (1976) stars and transformed the b-y values using the relation V-I = -0.00395 + 2.071846 (b-y) -1.09643 (b-y)^2 + 0.631039 (b-y)^3 obtained from 122 E-region secondary standards of Cousins (1976, 1987). Some of the stars also have measured V-I values (Cousins 1980a,b; Bessell 1990a) and these were used in preference to the transformed ones.

Caldwell et al. (1993) have also derived polynomial relations to transform between UBVRIJHK and uvby. Such representations are very useful, but over the 10 mag range of V-K and 5 mag range of V-I such fitted polynomials are unable to recover the nuances of the original mean relation across the full color range. In such cases it is better to break up the whole range into several overlapping sections and fit each section separately. Although mean color-color relations can be used successively to transform colors for a homogeneous group of stars it is not good practise for stars with a range of stellar parameters and it is important to measure accurate BVRI colors for all the AAM96 stars, in particular the extreme subdwarfs.

When using or interpreting the colors of stars one should always be aware that the observed colors of stars are likely to be affected by interstellar reddening. Estimates of the reddening can be made in several ways. The most accurate way is to use a reddening independent colour or index such as the Q index for OB stars (see Appendix F) or the H_β index for F stars.

Another technique is to use maps of the galactic distribution of dust, such as those of Fitzgerald (1986) and Burnstein & Heiles (1982) combined with estimate of the distance of the star from a trigonometric parallax or spectral/luminosity class. However, it is generally believed that within 100 pc of the Sun the interstellar reddening is insignificant and many of the stars used to calibrate color-color and color-temperature relations are nearby. In fact, none of the stars that we used from the AAM96 list were reddened and only 7 of the stars used in BLG94 had (V-K) reddenings larger than 0.02 mag. A comparison of the Yale and Hipparcos parallaxes for the 15 stars with reddening between 0.02 and 0.04 mags showed that Hipparcos moved six of the stars closer and five further away. Looking at the residuals to the fit between $T_{\rm eff}$ and color and correlating with the new distances showed that some of the reddenings did appear to be overestimated. However, as the reddenings were already quite low, the calibration scarcely changed. BLG94 show in their Table 13 the effect of interstellar extinction on angular diameters for a range of temperatures.

The Hipparcos parallax database when combined with photometric catalogs and the Burstein & Hailes maps should enable the production of much better maps of reddening versus distance than previously available, thus permitting better reddening corrections for more distant stars.

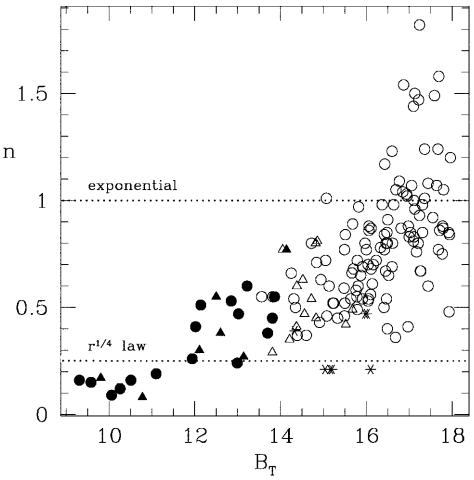

Fig. 2. Empirical $T_{\rm eff}$ versus V-I relation for dwarfs. Solid symbols are data from BLG94; crosses indicate AAM96 (for -0.2 < [Fe/H] < 0.2); open circles with error bars indicate Code et al. (1976)

Fig. 2 shows the $T_{\rm eff}$ versus V-I diagram using IRFM temperatures from BLG94 and AAM96 (for -0.2 < [Fe/H] < 0.2) together with the intensity interferometer measurements of Code et al. (1976) for A-F stars. The IRFM data yield higher precision for the A-F stars than did the intensity interferometer measures but the results show good agreement except for the hottest stars in the IRFM data and HR7557 of Code et al.

By good fortune, the mean empirical temperature scale for A-M stars has not changed appreciably from that summarised by Bessell (1979) although the precision of empirical temperature derivations has greatly improved over the past 16 years. The most significant improvements have occurred in the model atmospheres, in the computation of more realistic line blanketed spectra which permit better broad-band colors to be synthesised and in the precision and accuracy of observed colors of stars from the UV to the IR.

In Table 7 are listed the coefficients for polynomial fits for giant stars between $T_{\rm eff}$ and V-K. The interferometer data were fitted alone then combined with the IRFM data. Table 8 lists the mean empirical $T_{\rm eff}$ versus V-I relation for A-K dwarfs.

In Table 9 for completeness we list the empirical temperature scale for the O and B stars adopted by Sung (1997) based on Crowther (1997) and Böhm-Vitense (1982).

3.2. Comparison between model atmosphere and empirical $T_{\rm eff}$ versus color relations

We compared empirical relations $T_{\rm eff}$-(U-B), $T_{\rm eff}$-(V-K), $T_{\rm eff}$-(V-I), $T_{\rm eff}$-(I-K) for dwarfs and $T_{\rm eff}$-(V-K) for giants with the corresponding theoretical relations. We discuss the ranges 50000 - 10000K for (U-B), 4500-9500K for dwarfs and 2600-5000K for giants for (V-K), 9500-2000K for (V-I), and 4500-1500K for (I-K).

We derive the relevant test gravities for our models in the following way. Most of the A-G stars used by BLG94 and AAM96 for their IRFM calibration are in the Yale parallax catalog so one

Table 7. Polynomial fits to empirical $T_{\rm eff}$ versus V-K relations for giants.
$T_{\rm eff}$ = M0 + M1*(V-K) + M2*(V-K)^2 +...

Data sets	M0	M1	M2	M3	M4	M5	min	max
bcd	9102.523	-3030.654	633.3732	-60.73870	2.135847		2.00	10.0
abcd	9037.597	-3101.282	717.7044	-85.83809	5.021194	-0.1137841	1.50	10.0

(a) Blackwell & Lynas-Gray (1994) (b) Di-Benedetto & Rabbia (1987) (c) Dyck et al. (1996) (d) Perrin et al. (1997)

Table 8. Polynomial fit to empirical $T_{\rm eff}$ versus V-I relations for A-K dwarfs
$T_{\rm eff}$ = M0 + M1*(V-I) + M2*(V-I)^2 +...

M0	M1	M2	M3	M4	M5	min	max
9581.1	-14264	40759	-74141	60932	-18021	0.0	1.0

Blackwell & Lynas-Gray (1994); Alonso et al. (1996); Code et al. (1976)

Table 9. Empirical $T_{\rm eff}$ versus Spectral Type and U-B relation for OB dwarfs from Sung (1997), Crowther (1997), and Böhm-Vitense (1982)

$T_{\rm eff}$	Sp	U-B	$T_{\rm eff}$	Sp	U-B	$T_{\rm eff}$	Sp	U-B	$T_{\rm eff}$	Sp	U-B
50000	O3	-1.22	30850	O9.5	-1.11	21380	B2	-0.85	12735	B7	-0.41
44000	O4	-1.20	29800	B0	-1.07	18750	B3	-0.75	11614	B8	-0.30
43000	O5	-1.19	28500	B0.5	-1.03	16866	B4	-0.66	10666	B9	-0.19
42000	O6	-1.18	26600	B1	-0.97	15346	B5	-0.58	9886	A0	-0.01
31800	O9	-1.12	24400	B1.5	-0.91	13932	B6	-0.50			

can estimate their luminosities and gravities. (Most of the stars will eventually have higher precision parallaxes from the Hipparcos database). This shows that few of the A-F stars observed are ZAMS stars and on the average they lie about 1 magnitude brighter than the ZAMS. An average gravity therefore should be between 3.5 and 4.

The relevant gravities and temperatures can also be well deduced for giants and dwarfs from theoretical isochrones (eg. Bertelli et al. 1994) and evolutionary tracks (eg. Schaller et al. 1992; Schaerer et al. 1993a,b; Charbonnel et al. 1993). Figs. 3a and 3b show the near main sequence and giant branch evolutionary tracks for 1, 1.5, 2.5, 5, 9, 15$M_\odot$ solar abundance (Z = 0.02) models from Schaller et al. (1992) supplemented by extensions to cooler temperatures by Bessell et al. (1991). Similar plots can be made for other abundances. The gravities of stars on the solar abundance giant branch range from log g = 3.0$\pm$ 0.5 near 5000K to log g = -0.2$\pm$ 0.5 at 3000K. ZAMS stars with spectral-types between O and late-F will have gravities between log g= 4.1- 4.2 .

In Fig. 4 we show the U-B versus $T_{\rm eff}$ relation from the OB dwarf models and from the empirical temperature scale of Crowther (1997). The agreement is excellent for temperatures below 30000K. However, for the hottest stars, ground-based UBVRI photometry is not recommended for accurate temperature determination and fluxes measured further into the UV such as with the WPFC2 filters F160BW are better to use. In a future paper we will present colors for the F160BW passband.

Figs. 5a and 5b compare the observed and theoretical V-K and V-I color-temperature relations for A-G dwarfs. Empirical (V-K)-$T_{\rm eff}$ data are from BLG94 and AAM96 while the (V-I)-$T_{\rm eff}$ relation shown (Table 8) was the line fitted to the data in Fig. 2. The model atmosphere colors are for the no-overshoot ATLAS9 models for three values of log g= 3.5, 4.0, 4.5. Although these no-overshoot model colors being a little bit bluer fit the observations better than the overshoot models do, the V-K and perhaps the V-I still appear a little too red also for log g included between 3.5 and 4.0, which roughly corresponds to that of the calibrating stars.

Such a small difference could result from the adopted model and colors for Vega and Sirius used to fix the zero points, from remaining problems with the models or from passband mismatches. Nevertheless, with a small adjustment the theoretical colors are in excellent agreement with the observations.

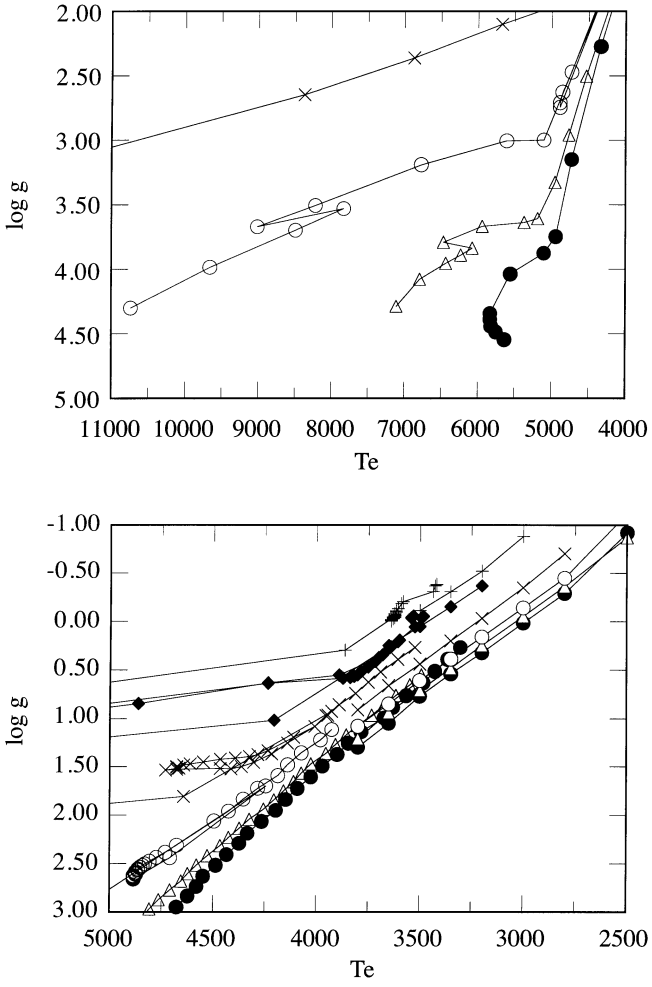

Fig. 3. a Theoretical evolutionary tracks near the main sequence for 1 (filled circles), 1.5 (triangles), 2.5 (open circles), 5 (crosses) $M_\odot$ models with Z = 0.02 from Schaller et al (1992). **b** Theoretical giant branch tracks for 1 (filled circles), 1.5 (open triangles), 2.5 (open circles), 5 (crosses), 9 (filled diamonds) and 15 (pluses) $M_\odot$ models with Z = 0.02 from Schaller et al (1992) together with extensions to higher luminosities and cooler temperatures from Bessell et al. (1991).

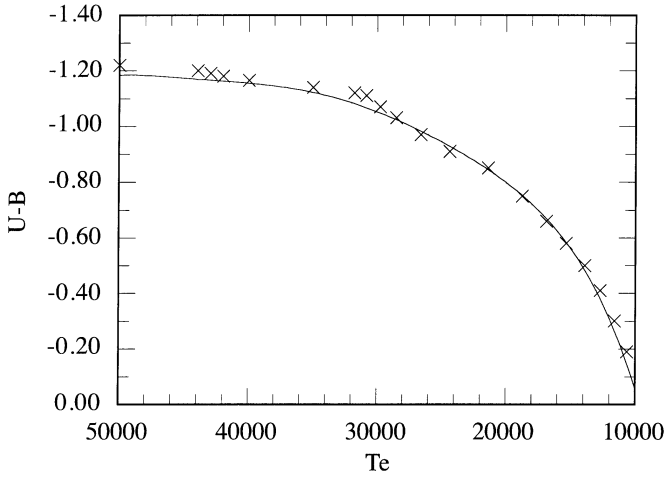

Fig. 4. The $T_{\rm eff}$ versus U-B diagram from the model atmospheres (full line) compared with the empirical relation from Crowther (1997) (crosses)

Fig. 6 compares empirical and computed V-I versus $T_{\rm eff}$ relations for the G - M dwarfs. IRFM temperatures are available for some G-K dwarfs (BLG94, AAM96, Tsuji et al. 1995, 1996), but only two eclipsing binary M dwarfs, YY Gem (Leung and Schneider 1978; Habets & Heintze 1981) and CM Dra (Lacy 1977) have measured radii. YY Gem is an old disk star with near-solar abundances but CM Dra is a high velocity star although its spectrum does not indicate an obviously large metal deficiency. Chabrier & Baraffe (1995) have recently discussed both systems. The Plez (1997) NMARCS model colors (Table 6) appear a good match to the eclipsing binaries temperature scale and seem to indicate convergence with the ATLAS9 models at 4250K. For the log g = 4.5 solar abundance grid the Brett (1995a,b) colors computed with the older opacities set (Table 6) show a V-I smaller by about 0.07 at 3800K, increasing to 0.4 at 3000K and to 1.0 at 2400K.

The ATLAS9 no-overshoot model colors are a good representation of the colors of the hotter dwarfs. However, one should note that an earlier paper by Leung & Schneider (1978) derived an effective temperature of 3770K for YY Gem about 300K cooler than that used here and in addition, Chabrier & Baraffe (1995) suggest that CM Dra could be 3300K (150K hotter).

Empirical and theoretical (I-K)-$T_{\rm eff}$ relations for M dwarfs are compared in Fig. 7. The ATLAS9 dwarf models are indicated by the upper line and the Plez (1997) dwarf relation by the lower line. Here in addition to YY Gem and CM Dra (open circles) are shown the IRFM temperatures for some M dwarfs from Tsuji et al. (1996a) (crosses) and fits to far-red spectra by Brett (1995a) (filled circles). As seen for V-I, the model $T_{\rm eff}$ versus I-K relations are in quite good agreement with the observations. The advantage of using the I-K color for cool M dwarfs is that it continues to increase monotonically with decreasing temperature unlike the observed V-I color which becomes bluer in the latest M dwarfs. They are in good agreement with Tsuji's IRFM temperatures around 2000K.

In Fig. 8 we compare the observed and the model $T_{\rm eff}$ -(V-K) color relations for the GKM giants. The plotted observational data are from BLG94, Di Benetto & Rabbia (1987), Dyck et al. (1996) and Perrin et al. (1997). The continuous line is the mean empirical relation discussed in Sect. 3.1. The model colors are in extremely good agreement with the observations even given the complication of a range in model color depending on gravity and extension. For temperatures between 4000K and 3400K the effect of mass (or sphericity) is comparable or greater than the effect of gravity on the V-K color but below 3200K the effect of gravity is very great. However, the expected log g for M giants (old disk) at around 3200K is about 0.25. Lower gravities are more typical of supergiants.

In Fig. 9 we show the difference between the empirical V-K versus $T_{\rm eff}$ relation and the theoretical NMARCS and ATLAS9 $T_{\rm eff}$ versus V-K color relation appropriate (solar abundance, $T_{\rm eff}$ and log g for a 1.5 $M_\odot$ track) for old disk giant branch stars.

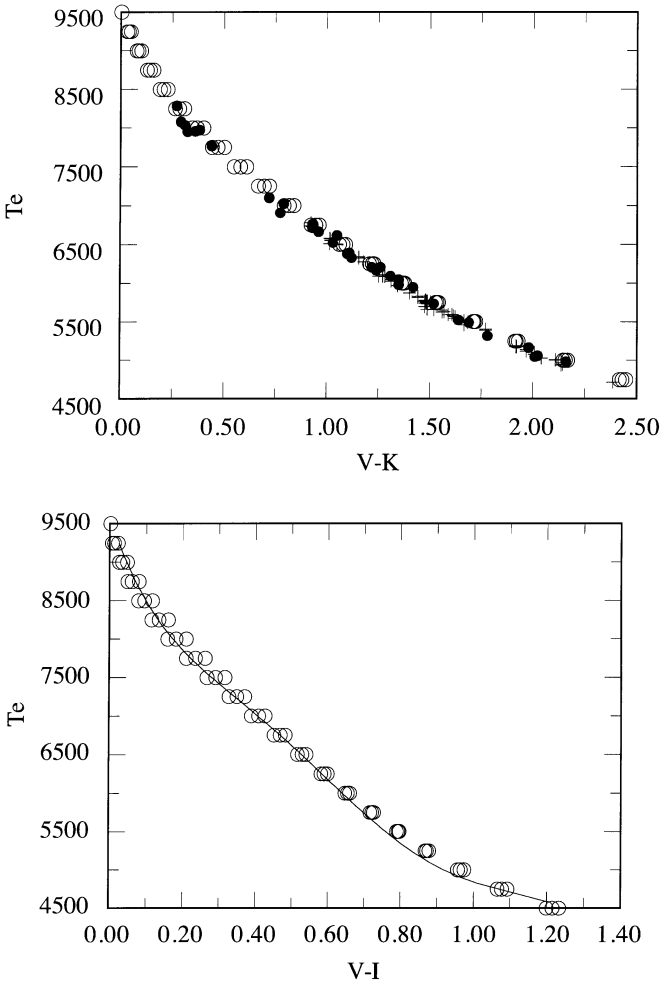

Fig. 5. a $T_{\rm eff}$ versus V-K relation from the model atmospheres compared with the empirical relation from the IRFM method for A-G dwarfs taken from BLG94 and AAM96. Symbols for observations are as in Fig. 2. **b** $T_{\rm eff}$ versus V-I relation from model atmospheres compared with the polynomial fit to the empirical $T_{\rm eff}$ versus V-I relation for A-K dwarfs given Table 8. In both figures **a** and **b** open circles are the colors from ATLAS9 no-overshoot models (Table 2). They are plotted for log g = 4.5, 4.0, 3.5; higher gravity gives redder color

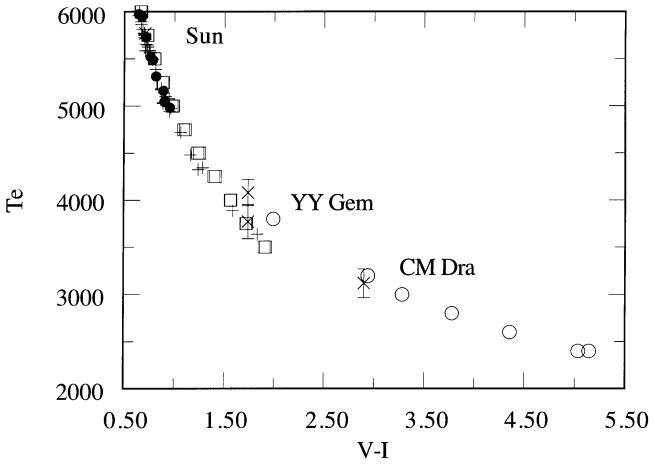

Fig. 6. Comparison between model and empirical $T_{\rm eff}$ versus V-I colors for G-M dwarfs. The dwarfs with IRFM temperatures are plotted as filled circles BLG94 and plus signs (AAM96). The dwarfs with directly measured radii (large crosses with error bars) are the Sun and the eclipsing binaries YY Gem and CM Dra. The ATLAS9 no-overshoot models for log g =4.5 and 4.0 are indicated by open squares; the open circles are the NMARCS models for log g = 4.5

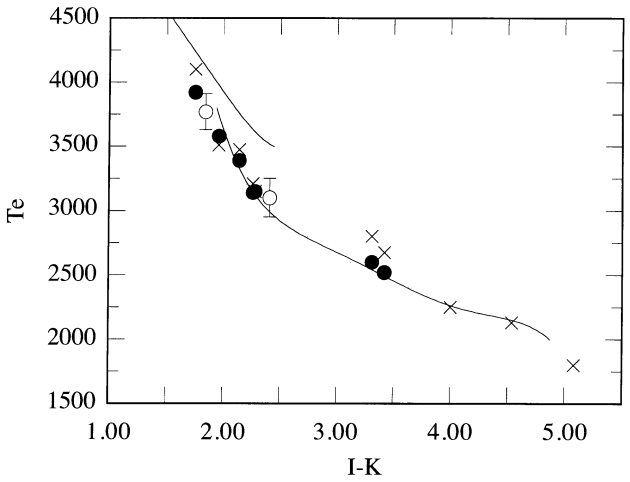

Fig. 7. The comparison between model and empirical $T_{\rm eff}$ versus I-K color for M dwarfs. The open circles with error bars are YY Gem and CM Dra; the crosses are IRFM data from Tsuji et al. (1995, 1996); the filled circles are Brett (1995a) fits to far-red spectra. The upper line represents the no-overshoot ATLAS9 models of Table 2, the lower line represents the Plez (1997) NMARCS models of Table 6.

The error bars indicate the Michelson interferometer data. The remaining points are from BLG94. The open circles indicate the residual to the spline fit to the ATLAS9 and NMARCS data. It is clear that the agreement is excellent, although there seems to be small systematic difference of about 50K near 5000K.

3.3. Comparison between model atmospheres and empirical color-color relations

Empirical relations are compared with theoretical relations for (J-K,V-K), (V-I,V-K), and (B-V,V-I) indices for both dwarfs and giants. $T_{\rm eff}$ ranges from 5000 to 2500K for (J-K, V-K); from 9500K to 2500K for dwarfs and from 5000K to 2800K for giants for (V-I,V-K); from 9500K to 2500K for dwarfs and from 4000K to 2500K for giants for (B-V,V-I).

Fig. 10 compares the observed and theoretical J-K versus V-K diagram for $T_{\rm eff} \leq$ 5000 K . The upper line represents the locus of the nearby giant stars, the lower line the dwarfs. The NMARCS and ATLAS9 giant model colors are in a good agreement with each other and with the observed locus for temperatures hotter than 4250K (V-K $<$ 3.0). Below 4000K (V-K $>$ 3.5) the NMARCS models better fit the observations. The ATLAS9 dwarf models (plotted as solid squares) lacking H_2O opacity do not fit the J-K color at all for temperatures below 4250K and the NMARCS models whilst showing the correct trend with temperature, obviously compute too strong H_2O bands. Brett

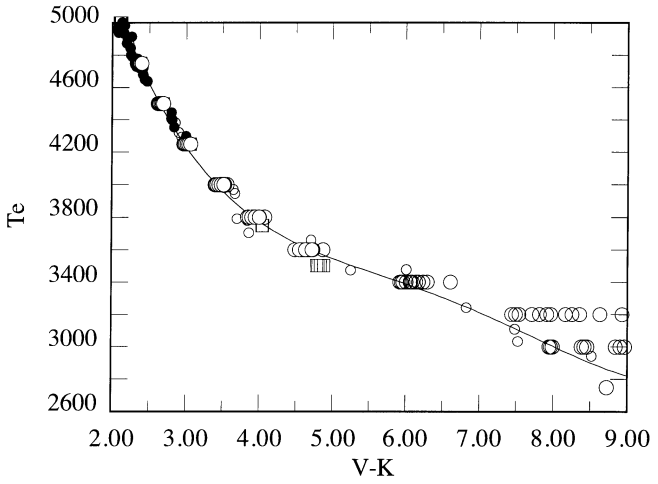

Fig. 8. Comparison between model $T_{\rm eff}$ versus V-K colors and the IRFM and interferometer temperatures for GKM giants . The closed circles are IRFM data; the small open circles are Michelson interferometer data. The open squares are ATLAS9 no-overshoot model colors from Table 2 for log g = 0.0, 0.5, 1.0, 1.5; the large open circles are NMARCS models for the same gravities from Table 4 and Table 5. Table 5 also gives colors for a range of extensions appropriate for 1 to 5 $M_\odot$ giants.

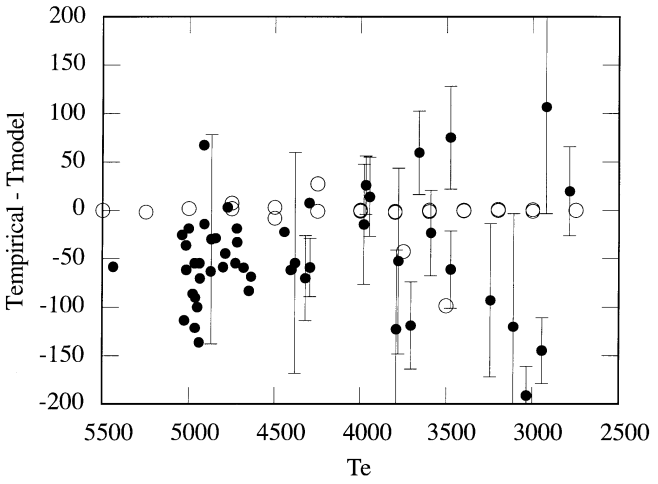

Fig. 9. The difference between the empirical and theoretical $T_{\rm eff}$ versus V-K for old disk giants. The data with error bars are the interferometer measurements. The other points are IRFM estimates. The open circles indicate the residuals to the spline fit to the NMARCS and ATLAS9 models.

(1995a,b) used as an H_2O line list derived from a statistical treatment of empirical mean opacity and line separation data for these preliminary models. The Plez (1997) models incorporate a better ab initio line list from Jørgensen (1996), which still does not provide a better fit to the observations in J-K. In the NMARCS grid currently being computed, H_2O opacity will also be incorporated on the basis of the very extensive line list from Partridge & Schwenke (1997) and we anticipate better although not perfect agreement. We suspect water vapour is not the only factor responsible for the bad fit in J-K. In addition, modelling of the atmospheres of the *coolest* M dwarfs may require the inclusion of grain opacities and an understanding of how grains form and segregate (see Tsuji et al. 1996b).

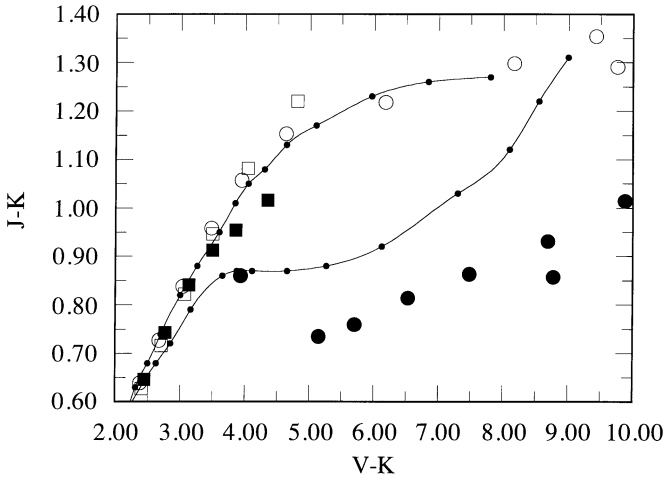

Fig. 10. Comparison between the observed and theoretical J-K versus V-K diagram. The small filled circles joined by a line represent the mean colors of nearby stars with spectral types from K0 to M7 for giants (upper line) and K2 to M7.5 (M10: Boeshaar 1976) for dwarfs (lower line) taken from Bessell & Brett (1988) and Bessell (1991). The ATLAS9 no-overshoot model colors (Table 2) are indicated by open squares (log g = 3.0 - 1.0) and filled squares (log g = 4.0, 4.5). The open circles are NMARCS giants from Tables 4 and 5. The filled circles are Plez (1997) NMARCS dwarfs from Table 6.

Fig. 11 shows the good agreement between the observed and computed V-I versus V-K colors for dwarfs, although this may be coincidence given the uncertainties that we know still exist in the line opacities. The observed turnover in the V-I colors are not shown by the coolest models. Fig. 12 shows that the agreement is excellent for M giant stars with temperatures below 4000K. The disagreement was large with the original colors from both NMARCS grids. With the old opacities the V-I color was too blue by a full magnitude around V-K = 7.

B-V is a color which does not agree well between observation and theory especially for cool stars. Fig. 13 and Fig. 14 show the B-V versus V-I relation for dwarfs and giants respectively. For the A-G dwarfs the agreement is reasonable although the synthetic B-V is slightly too red for the A-F stars. But for the M dwarfs the agreement is poor, the synthetic colors being 0.2 to 0.8 mags bluer than observed. For the giants (Fig. 14) the computed colors, in particular the NMARCS models, are also seen to be too blue by a few hundredths at 4750K and increasing to almost 0.2 mag at 3600K. Part of this may be due to the range in metallicity in the field stars; however, it mainly reflects the opacity incompleteness in the blue and UV. The NMARCS model V band flux has greatly improved (i.e. decreased) with the inclusion of new opacities and the revision of older ones. All the opacities at shorter wavelengths have not yet been carefully checked. The final NMARCS model grid will incorporate atomic line data from the VALD (Piskunov et al. 1995) database supplemented by the latest Kurucz data for lines not appearing in VALD. The current NMARCS models used line data from

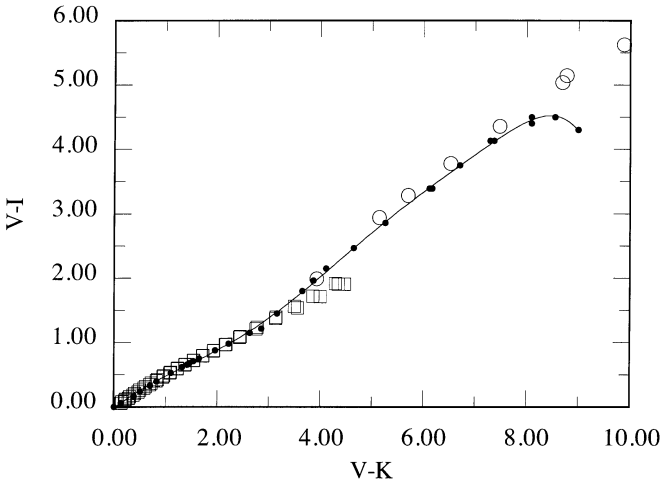

Fig. 11. Comparison of V-I versus V-K relations for dwarfs. The filled circles joined by a line represents the observed locus for solar-neighbourhood dwarfs from Bessell & Brett (1988) and Bessell (1991). The squares are ATLAS9 model colors from Table 2; the open circles the Plez (1997) NMARCS model colors of Table 6.

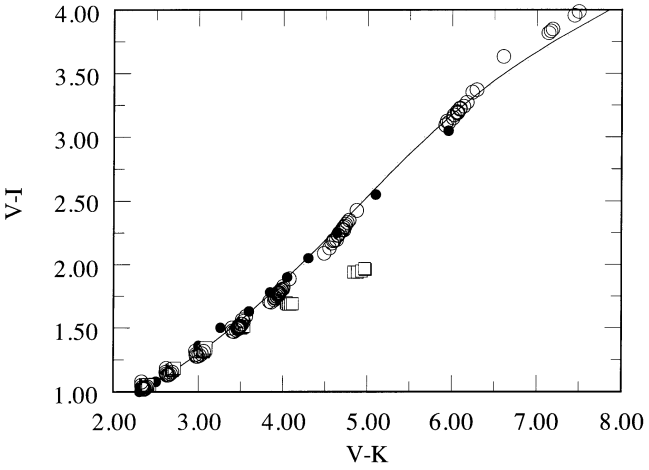

Fig. 12. Comparison of V-I versus V-K relations for giants. The filled circles are the observed locus for solar-neighbourhood giants from Bessell & Brett (1988) the line is the locus from Caldwell et al. (1993). The squares are ATLAS9 model colors from Table 2; the open circles the NMARCS model colors of Table 4 and 5.

an older Kurucz (1989) tape. It is worth noting also that many molecules have electronic transitions in the blue-UV region.

3.4. Abundance effects on color indices for KM giants

In the following Figs. 15 - 18, we show the effect of abundance on the B-V, V-I, V-K and J-K colors of KM giants. The abundances illustrated cover the range found in the centre of the Galaxy, the old and young disk and the Magellanic Clouds. We chose a set of temperature and gravity pairs appropriate for solar abundance old disk giants and used the same set of parameters for the different abundances. The plots therefore do not represent the giant branch loci for different abundances.

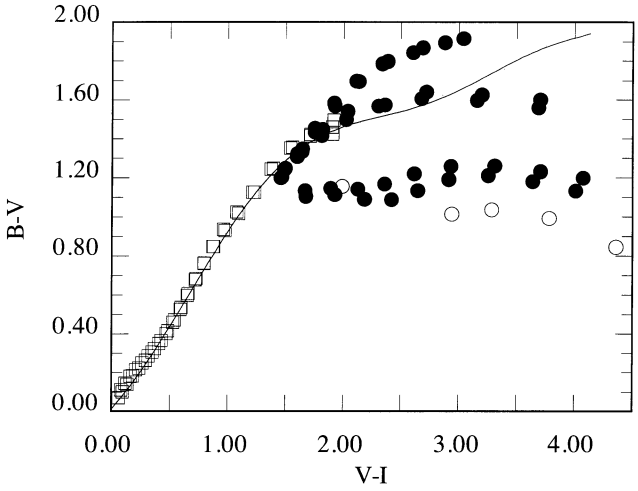

Fig. 13. Comparison of B-V versus V-I relations for dwarfs. The line is the observed locus from Caldwell et al (1993). The squares are ATLAS9 models colors (Table 2); the closed circles are the Brett (1995) NMARCS model colors (Table 6) for three metallicities, [M/H] = -2, -1 and 0; the open circles are the Plez (1997) NMARCS models for solar metallicity (Table 6).

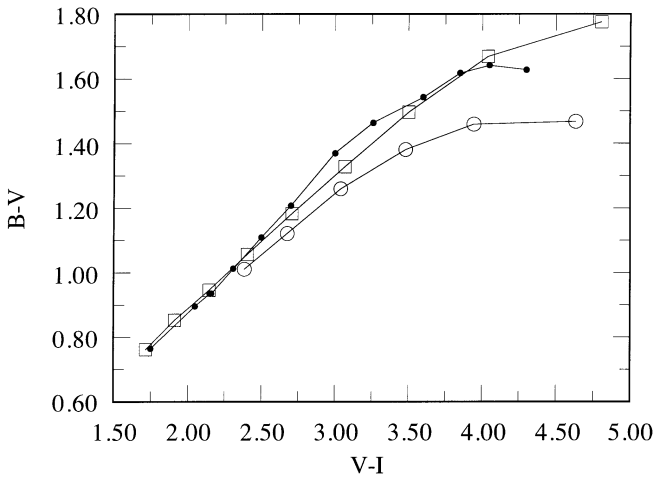

Fig. 14. Comparison of B-V versus V-I relations for giants. The line connecting the small dark points is the observed locus for G0-M2 stars from Bessell & Brett (1988). The squares are ATLAS9 models colors (Table 2) for ($T_{\rm eff}$, log g) = 3500, 0.5; 3750, 1.0; 4000, 1.5; 4250, 2.0; 4500, 2.5; 4750, 3.0; 5000, 3.5; 5750, 3.5; 5500, 4.0. The circles are the NMARCS model colors (Table 4 and 5) for ($T_{\rm eff}$, log g) = 3600, 0.5; 3800, 1.0; 4000, 1.5; 4250, 2.0; 4500, 2.5; 4750, 3.0.

For B-V, V-I and V-K decreasing metallicity means bluer colors (except in B-V for $T_{\rm eff} < 3900$K). However, J-K gets redder with decreasing metallicity. V-K is the least sensitive to metallicity and for temperatures greater than 4000K can be considered essentially independent of abundance.

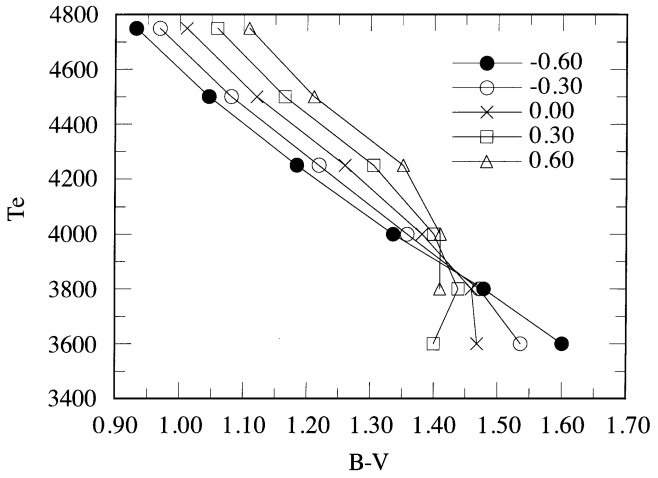

Fig. 15. The theoretical $T_{\rm eff}$ versus B-V relations for KM giants for parameters ($T_{\rm eff}$, log g) = 3600, 0.5; 3800, 1.0; 4000, 1.5; 4250, 2.0; 4500, 2.5; 4750, 3.0 and 5 metallicities, [M/H] = -0.6, -0.3, 0, 0.3, 0.6. NMARCS models (Table 5).

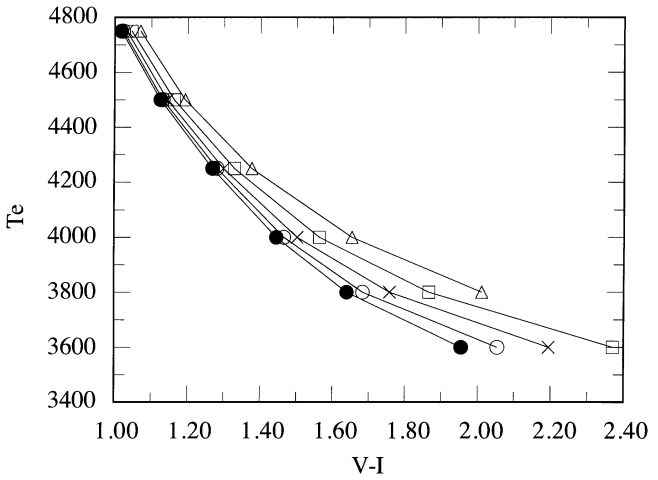

Fig. 16. The theoretical $T_{\rm eff}$ versus V-I relations for KM giants. Details and symbols as in Fig 15.

3.5. Comparison between model atmospheres and (V-I)-BC$_I$ and (I-K) - BC$_K$ empirical relations

Figs. 19a,b show the comparison between observed and computed bolometric corrections in I and K for dwarfs. The observed and model BC$_I$ are in good agreement except for the coolest models whose V-I colors are too red. The BC$_K$ are in excellent agreement. There is a small systematic difference between the Tinney et al. (1993) corrections and the model corrections. This is probably due partly to a slightly different adopted flux for Vega and Sirius and partly to the remaining model problems mentioned above. Finally, Fig. 20 also shows excellent agreement between the model and observed BC$_K$ for giants. The small difference for the coolest stars is certainly within the observational uncertainties and the model uncertainties. The NMARCS models of Table 5 shown in Figs. 15-18 have virtually identical BC$_K$ for different metallicities.

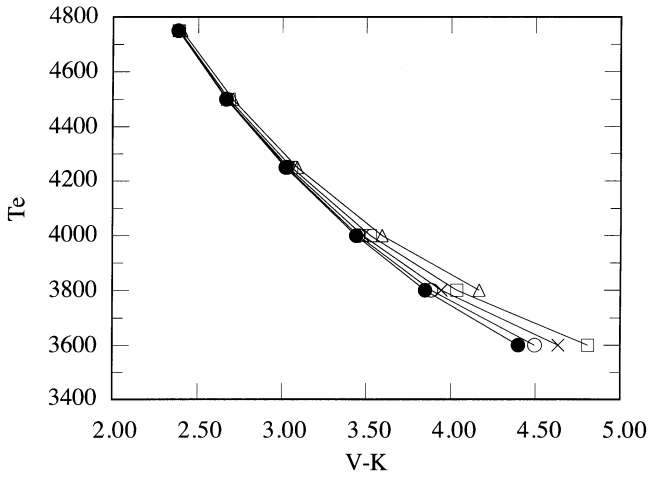

Fig. 17. The theoretical $T_{\rm eff}$ versus V-K relations for KM giants. Details and symbols as in Fig 15.

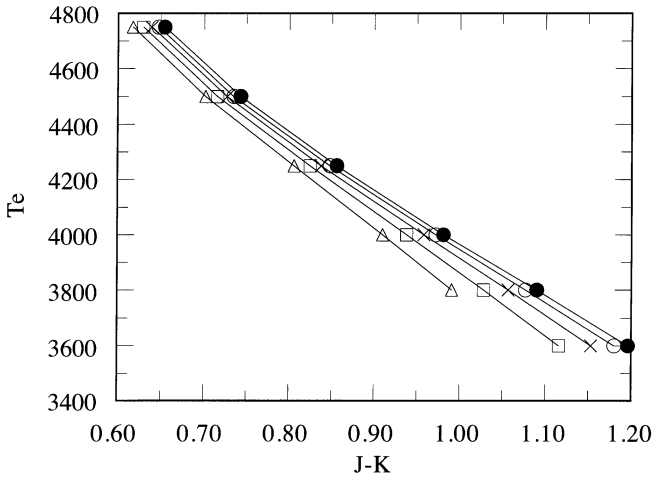

Fig. 18. The theoretical $T_{\rm eff}$ versus J-K relations for KM giants. Details and symbols as in Fig 15.

4. Conclusions

The new model colors and bolometric corrections have been compared with the empirical relations measured from stars in the solar neighbourhood. For most colors there is good agreement; in particular, the theoretical color versus $T_{\rm eff}$ relations for U-B for B0-A0 dwarfs, V-K for A-G dwarfs, V-I for A-M dwarfs, I-K for M dwarfs, and (V-K) for G-M giants are in excellent agreement with observations as are the theoretical and observed bolometric correction relations (V-I)-BC$_I$, (I-K)-BC$_K$ for dwarfs and (V-K)-BC$_K$ for giants.

The exceptions, for the NMARCS models, are the B-V indices for K giants, M dwarfs and M giants, and the J-K indices for M dwarfs cooler than about 2800 K. The reason for these differences needs to be examined, but problems in the IR of cool dwarfs are almost certainly due to a deficient line list for H_2O (Brett 1995a). For temperatures cooler than 2500K additional opacities due to grains and polyatomic molecules presumably become important and must also be included (see eg. Tsuji et

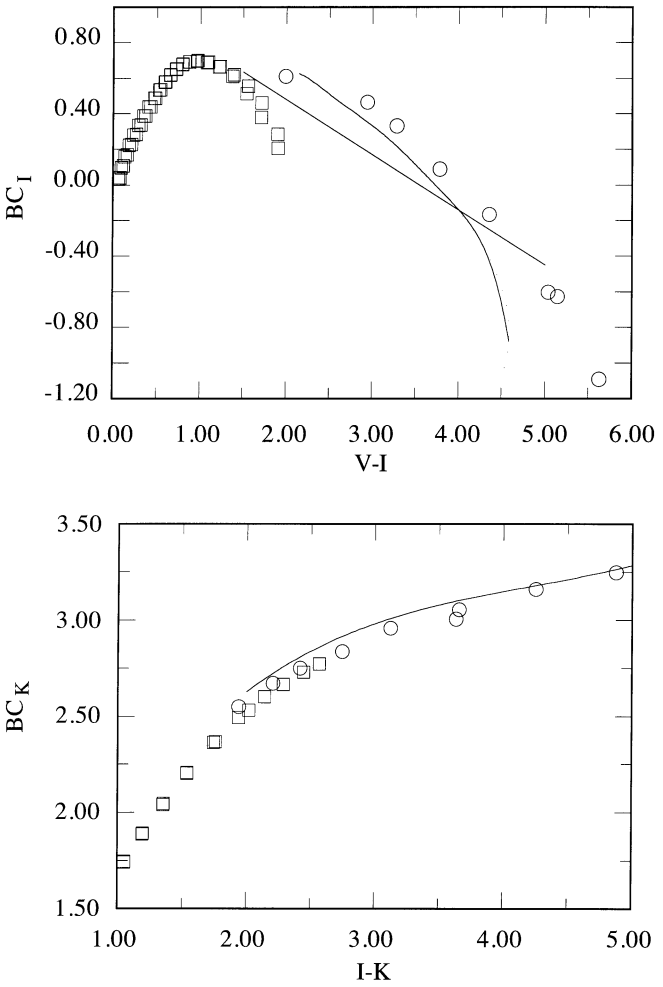

Fig. 19. a Comparison between the observed and theoretical I mag bolometric correction versus V-I for A-M dwarfs. The straight line is the relation given by Reid and Gilmore (1984) (adjusted for a different solar M_{bol}); the curved line is from Tinney et al. (1993). The squares are ATLAS9 model data for log g=4.5 (Table 2) and the open circles are Plez (1997) NMARCS model data (Table 6). **b** Comparison between the observed and theoretical K mag bolometric correction versus I-K for A-M dwarfs. The line is from Tinney et al. (1993). The squares are ATLAS9 model data for log g=4.5 (Table 2) and the open circles are Plez (1997) NMARCS model data for log g = 4.5 (Table 6).

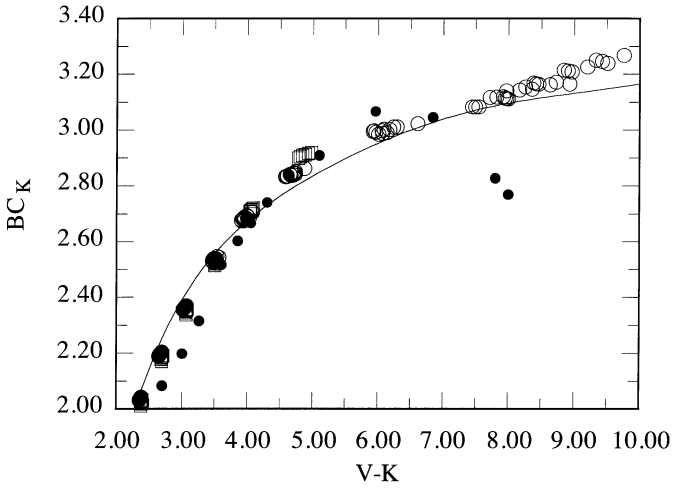

Fig. 20. Comparison between the observed and theoretical K mag bolometric correction versus V-K for KM giants. The line is from Bessell & Wood (1984); the filled circles are from Frogel et al. (1981). The squares are ATLAS9 giant model data (Table 2) and the open circles are NMARCS model data from Tables 4 and 5.

al. 1996a, b; Allard et al. 1996). Allard et al. (1994), Allard & Hauschildt (1995), Tsuji & Ohnaka (1995), and Tsuji et al. (1995) have also modelled cool M dwarfs and brown dwarfs. See also the first successful attempt by Chabrier et al. (1996) to derive an ab initio mass-luminosity (and colors) relationship for the bottom of the main-sequence, using Brett atmospheres as boundary conditions to evolutionary models.

Missing or erroneous opacities in the blue-visual region are probably mainly responsible for the (B-V) deficiencies. Detailed comparison of spectra rather than colors would be useful in this context. The present NMARCS models use, for the iron peak elements, the same atomic line lists used by Kurucz for computing line opacities (Kurucz, 1991). We then added a few strong lines of some other species. In addition to missing atomic line opacities, there is also the possibility that some molecular opacity sources are missing in the blue-visual region. Our inclusion of the TiO a-f system had a non-negligible impact on the V band as well as the inclusion of Langhoff's (1997) electronic transition momenta dependent of internuclear distance for the γ' transition system. Newer line lists merging a larger number of transitions taken from the most updated available data bases (Kurucz, 1995b; Piskunov et al., 1995) should show further improvements in the calculated fluxes.

Cooler than 3000K most M giant stars are variable and the regular shock waves that traverse the atmospheres create a greatly extended atmosphere. The static model atmospheres discussed in this paper cannot be expected to adequately represent the cooler giants. Investigatory models of such stars have been computed by e.g. Bessell et al. (1989, 1991, 1996) and Höfner & Dorfi (1997) . Bessell et al. (1991) have computed AGB tracks for red giants and supergiants that extend as cool as 2500K. Colors and luminosities were also published for these tracks but some of these broad-band colors are not as realistic as the colors presented here because of limitations in the line opacities and methods used. The model structures, however, may not be as affected. But in a recent work, Alvarez & Plez (1997) have computed very realistic colors for mira models with the NMARCS line opacities and these offer great prospects for the more realistic spectral modelling of miras. Scholz & Takeda (1987) discuss complications in radii measurements in such extended mira models.

The ATLAS9 models fit stars hotter than 4250K very well for all the indices examined. For cooler stars, the NMARCS models with their more complete molecular opacity are preferred to ATLAS models below 4200 K for M dwarfs, and below 4000 K for M giants. Giant model colors are very similar to the NMARCS colors for temperatures hotter than 4000K.

Also the Gustafsson et al. (1975) models were inadequate for temperatures below 4500K; in fact, they yielded systematically too low abundances for stars cooler than about 4300K when model parameters were derived from the observed colors and the Ridgway et al. (1980) temperature scale (Bessell 1992). Using the NMARCS models, Bessell & Plez (1997) find no systematic trends in abundance with temperature along the giant branch in M67 and 47 Tuc. The V-K and V-I colors show little sensitivity to gravity between 6000 and 4000K. For temperatures below 3600K, lower gravity models are much redder and more extended (lower mass) models are a little redder.

On the basis of above comparisons one could expect that the model colors for different abundances, luminosities and masses should enable equally as reliable temperatures to be derived for stars of all mass and age (for very extreme cases, like very metal-poor stars more tests will be needed as different opacity sources manifest themselves). We can further expect that excellent integrated colors for clusters and galaxies can be computed by using the theoretical effective temperature-effective gravity loci from theoretical isochrones and evolutionary tracks and interpolating colors from the new model atmosphere grids.

Acknowledgements. Part of this work was accomplished while BP held an EU HCM Fellowship at the Niels Bohr Institute, Denmark. BP warmly thanks B. Gustafsson at Uppsala Astronomical Observatory for continuous support, through various NFR, DFR and Crafoord grants, and encouragement and S. Johansson for his hospitality at the atomic spectroscopy division at Lund University.

Appendix A: zero-points of the broad-band synthetic photometric system

The zeropoints of the UBVRIJHKL broad band system have been traditionally set by using the magnitude and color of Vega or a set of A0 stars. However, because Vega is not in the precise photometric catalogs of Cousins (UBVRI) and Glass-Carter (JHKL) being unobservable from the southern hemisphere and because some doubts have been expressed about its variability and possible IR excess, it was decided (following Cohen et al. 1992) to adopt Sirius as an additional fundamental color standard. We have therefore chosen to use the observed V magnitude of Vega as defining the V zeropoint, but the observed colors of Sirius together with the colors of Vega and the synthetic magnitudes of the ATLAS models of Vega and Sirius to define the zero-points for the other bands. The adopted models for Vega and Sirius have the parameters ($T_{\rm eff}$, log g, Z, v_{micro}) = 9550K, 3.95, [-0.5], 2kms^{-1} (Castelli & Kurucz 1994) and 9850K, 4.25, [+0.5], 2kms^{-1} (Kurucz, 1997).

A.1. The zeropoint for V

Using the Vega model from Castelli & Kurucz (1994) we derived the following relation between standard V magnitudes and the computed absolute fluxes at the earth in the V band:

$$V = -2.5 \log (\int f(\lambda) R_V(\lambda) d\lambda)/(\int R_V(\lambda) d\lambda) - 21.100$$

$$V = -2.5 \log (\int f(\nu) R_V(\nu) d\nu)/(\int R_V(\nu) d\nu) - 48.598$$

where $R_V(\lambda)$, $R_V(\nu)$ are the V response function (eg. normalised passbands from Bessell 1990) and $f(\lambda)$ and $f(\nu)$ are the computed flux at the earth in erg cm^{-2} s^{-1}Å^{-1} or in erg cm^{-2}s^{-1} hz^{-1} respectively. The above zeropoints realize a V magnitude of 0.03 mag for Vega.

We note that the absolute flux at 5556Å of the Vega model and the observed flux for Vega (Hayes 1985) are in good agreement and consistent within the 1 sigma error bars of the angular diameter measurements (Code et al. 1976). For Vega: $q_d = 3.24 \pm 0.07$ mas, the model implies 3.26 mas. For Sirius: $q_d = 5.89 \pm 0.16$ mas, the model used by Cohen et al. (1992) implies 6.04 mas. It is anticipated that new Michelson measurements and parallaxes will improve the precision of the angular diameters and effective temperatures for Vega and Sirius and permit better model fittings and comparisons.

A.2. The color indices zeropoints

To derive the zero points for U-B, B-V, V-R, and V-I color indices we averaged the differences between the observed and computed colors for Vega and Sirius. The zero points for the V-J, V-H, V-K, and V-L colors were derived by fitting the observed indices of Sirius.

In Table A1 are given the observed colors and magnitudes together with the synthetic colors and the zeropoints for the synthetic color indices. In general there is excellent agreement between the observed and computed colors for Vega and Sirius. There is somewhat larger disagreement between the observed and computed V-K color for Vega, but it is well within the standard errors of the 1966 Johnson IR catalog.

The IR magnitudes for Sirius (Glass 1997; private communication) were measured in the current standard SAAO system by Carter (1990). The zero-point of the current SAAO system was determined from observations of 25 main-sequence stars between B1 and A7 spectral type. The zero-point of K was set by plotting V-K against B-V for the 25 stars and ensuring that the locus passed through V-K= 0 for B-V= 0. Zero-points and color terms for the ESO, CTIO, AAO and the MSSSO systems relative to the SAAO system are also given in Carter (1990).

The possible IR excess for Vega has been investigated by Leggett et al. (1986) who measured the narrow-band 1-5μ magnitudes for 25 dwarfs of spectral-type B8-A3 relative to Vega. They found that (the asterisk refers to the narrow band index) the (V-J*, J*-K*, J*-L*, J*-M*) = (0.03, 0.006, 0.019, 0.023) colors of Vega were normal for an A0 star and if anything, 1-2 percent fainter between K* and M* than the mean A0 star; that is, Vega does not have an IR excess *compared to other A stars*.

However, the absolute infrared flux calibrations of Vega by Mountain et al. (1985), Blackwell et al. (1983) and Selby et al. (1983) have shown Vega to have an excess between 2 and 5 μm relative to model spectra by Dreiling and Bell (1980) and by Kurucz (1979), which led Leggett et al (1986) to suggest that the theoretical infrared flux from A-type stars is in error. This would be difficult to understand as the dominating H opacity in

Table A1. Observed and model colors for Sirius and Vega

	V	U-B	B-V	V-R	V-I	V-K	J-K	H-K	K-L	Ref
Sirius	-1.43	-0.045	-0.01							Cousins 1972
	-1.42			-0.012	-0.020					Cousins 1980c
	-1.43		0.00	-0.01	-0.016					Bessell 1990
	-1.43					-0.061	-0.018	-0.009	0.003	Glass 1997
Model	-1.38	-0.040	-0.008	-0.013	-0.021	-0.061	-0.018	-0.009	0.003	This paper
Vega	0.03		-0.01	-0.009	-0.005					Bessell 1990
	0.03	0.00	0.00			0.02	0.01		0.01	Johnson 1966*
Model	0.03	-0.004	-0.002	-0.007	-0.003	0.00	-0.003	-0.001	0.008	This paper†
zp		-0.454	0.606	0.548	1.268	4.906	2.247	1.145	1.877	

* IR colors transformed using Bessell & Brett 1988
†Adopted V magnitude for Vega

A stars is thought to be very well known. It is more likely that there remains a problem with horizontal and vertical extinction corrections in the absolute flux measurements. Eitherways, until this is understood it is recommended that the theoretical fluxes of model atmospheres, such as those for Sirius and Vega be used for absolute flux calibration through the atmosphere (see also Cohen et al. 1992).

Appendix B: zeropoint fluxes for the UBVRIJHKL system

In Table A2 are given the mean fluxes and the zeropoints corresponding to a fictitious A0 star with a magnitude of zero in all bands. These are based on V = 0.03 mag for Vega discussed above.

Appendix C: colors of the sun and solar analogs

The sun has also often been used for flux and magnitude calibrations. There have been several direct measurements of the solar V and B magnitudes. One of the most respected is that of Stebbins & Kron (1957). From their paper, using recent standard V magnitudes for their comparison G dwarfs one deduces V = -26.744 $\pm$ 0.015 for the sun. Hayes (1985) claims a further 0.02 mag correction for horizontal extinction yielding V = -26.76 $\pm$ 0.02. Other direct solar measurements have been discussed by Hayes (1985).

Direct spectrophotometric observations of the sun have also been made, Neckel & Labs (1984) work on the visual spectrum being the best known. These have been well discussed by Colina et al. (1996) who have derived a combined flux spectrum (solar_reference) for the sun between 0.12μm and 2.4μm. We have computed magnitudes and colors for that spectrum and these are given in Table A3.

The colors of the solar analogs have also been used for assessing solar colors. Hardorp (1980) was amongst the first to propose a list of stars whose spectra resembled that of the sun; however, the latest word is that of Cayrel de Strobel (1996) who has carefully compared hydrogen line profiles and derived temperatures, gravities and abundances for a list of possible candidate analogs. In Table A3 we give the mean U-B and B-V of the stars in her Table 6. The other colors were derived from the "solar" R-I = 0.337 (Taylor 1992) using mean color-color relations for G dwarfs from data in Allen & Tinney (1991), Carter (1990) and Bessell & Brett (1988).

Finally, we have also synthesized colors and magnitudes for the ATLAS9 model atmospheres of the sun computed with the overshooting option switched both on (SUN-OVER) and off (SUN-NOVER) (Castelli et al. 1997).

There is generally good agreement between the observed, solar analog and synthetic colors with the exceptions of U-B and V-I. The agreement in the absolute flux level is excellent although other attempts at direct solar flux measurements show larger scatter (eg. see Hayes 1985). We will adopt V = -26.76 for the sun which corresponds to M_V = 4.81 for a distance modulus of -31.57.

Appendix D: bolometric corrections and the zeropoint of the bolometric magnitude scale

The definition of apparent bolometric magnitude is

$$m_{bol} = -2.5 \log(f_{bol}) + \text{constant}$$
or
$$m_{bol} = -2.5 \log(\int f_\lambda d\lambda) + \text{constant}$$

where f_{bol} is the total flux received from the object, outside the atmosphere. The usual definition of bolometric correction

$$BC_V = m_{bol} - m_V$$

is the number of mags to be added to the V magnitude to yield the bolometric magnitude. The value of BC_V does not change when magnitudes at the stellar surface or absolute magnitudes are considered. In fact they differ from the apparent magnitudes only for the distance, which is eliminated when the difference between the bolometric and V magnitude is taken.

Although originally defined for the V magnitude only, the definition has now been generalised to all passbands (hence the V subscript above). Although the definition of bolometric magnitude is a straightforward one, there is some confusion in the literature resulting from the choice of zeropoint. Traditionally it had been generally accepted that the bolometric correction

Table A2. Effective wavelengths (for an A0 star), absolute fluxes (corresponding to zero magnitude) and zeropoint magnitudes for the UBVRI-JHKL Cousins-Glass-Johnson system

	U	B	V	R	I	J	H	K	Kp	L	L*
λ_{eff}	0.366	0.438	0.545	0.641	0.798	1.22	1.63	2.19	2.12	3.45	3.80
f_ν	1.790	4.063	3.636	3.064	2.416	1.589	1.021	0.640	0.676	0.285	0.238
f_λ	417.5	632	363.1	217.7	112.6	31.47	11.38	3.961	4.479	0.708	0.489
zp(f_λ)	0.770	-0.120	0.000	0.186	0.444	0.899	1.379	1.886	1.826	2.765	2.961
zp(f_ν)	-0.152	-0.602	0.000	0.555	1.271	2.655	3.760	4.906	4.780	6.775	7.177

f_ν (10^{-20} ergs cm^{-2} sec^{-1} hz^{-1})
f_λ (10^{-11} ergs cm^{-2} sec^{-1} Å^{-1})
mag_λ = -2.5 log (f_λ) - 21.100 - zp(f_λ)
mag_ν = -2.5 log (f_ν) - 48.598 - zp(f_ν)

Table A3. Observed and model magnitudes and colors for the Sun and a mean solar analog

	V	U-B	B-V	V-R	V-I	V-K	J-K	H-K	Ref
Sun	-26.76								Stebbins & Kron 1957
Sun_ref	-26.75	0.128	0.649	0.370	0.726	1.511	0.372	0.039	Colina et al. 1996
Analog		0.185	0.652	0.355	0.692	1.50	0.38	0.045	Cayrel de Strobel 1996; Table 6
Model	-26.77	0.135	0.679	0.367	0.725	1.524	0.373	0.041	SUN-OVER
Model	-26.77	0.145	0.667	0.361	0.715	1.524	0.376	0.032	SUN-NOVER

in V should be negative for all stars (but with generalisation of the correction to all passbands this rationale vanishes) and this had resulted in F dwarfs having a BC near zero and consequently the BC for solar-type stars was between -0.07 (Morton & Adams, 1968) and -0.11 mag (Aller, 1963). However, with the publication of his grid of model atmospheres, Kurucz (1979) formalised this tradition and based the zeropoint of his BC_V scale on the computed bolometric correction of a ($T_{\rm eff}$=7000, log g=1.0) model, which had the smallest BC in his grid, resulting in BC_V = -0.194 for his solar model. This zero-point based on model atmospheres was adopted by Schmidt-Kaler (1982) who assigned BC_V = -0.19 to the Sun.

Problems in the literature have occurred when BC_V tables have been used from various empirical and theoretical sources without addressing the different zeropoints involved. As emphasized by Cayrel (1997), the traditional basis of the zeropoint is no longer useful and we should adopt a fixed zeropoint, disconnected formally from other magnitudes, but related to fundamental solar measurements for historical reasons.

The solar constant is $f_{\odot tot}$ = 1.371 x 10^6erg cm^{-2}s^{-1} or 1371W m^{-2}s^{-1}(Duncan et al. 1982), therefore the total radiation from the sun $L_\odot$= 3.855(6) x 10^{33} erg s^{-1} and the radiation emittance at the sun's surface $F_\odot$ = 6.334 x 10^{10}erg cm^{-2}s^{-1}. The effective temperature is $T_{\rm eff}$= ($F_\odot/\sigma$)$^{1/4}$= 5781K.

Let us *define* the absolute bolometric magnitude of the sun $M_{bol\odot}$ = 4.74.

By adopting the *measured* apparent V magnitude of the Sun $V_\odot$ = -26.76, the absolute M_V magnitude of the sun is thus 4.81 and the V bolometric correction for the sun is then BC_V = 4.74 - 4.81 = - 0.07.

The absolute bolometric magnitude for any star with luminosity L, effective temperature T_{eff}, and radius R is then

M_{bol} = 4.74 - 2.5 log($L/L_\odot$)

M_{bol} = 4.74 - 2.5 log($T^4_{eff}R^2/(T^4_{eff\odot}R^2_\odot)$)

The computed V magnitude, whose expression was given in A1, transforms to M_V through:

M_V = V - 2.5 log(R^2/D^2_{10}),

where D_{10} is 10 parsecs. The bolometric correction follows:

BC_V = 4.74 - V - 2.5 log(T^4_{eff}) + 2.5 log(D^2_{10}) + 2.5 log($T^4_{eff\odot}R^2_\odot$).

And finally:
BC_V = -V - 2.5 log(T^4_{eff}) - 0.8737.

This expression was used to compute the bolometric correction of our models. By adopting the *synthetic* absolute $M_{V\odot}$ = 4.802, the V bolometric correction for the sun is then BC_V = 4.74 - 4.802 = - 0.062. This is very close to the above defined -0.07 and within the error bars of both observations and synthetic spectra in the V band. As models evolve with time and slight future changes in the calculated V magnitude cannot be excluded we chose not to rely on the solar model -0.062 bolometric correction but rather to keep the -0.07 value, with the adopted M_{bol} = 4.74 and the measured M_V = 4.81 V magnitude. This returns to the pre-Kurucz 79 value for the sun. Note that the V magnitude we adopted lies midway between the synthetic

Table A4. Comparison of tabulated solar V magnitude, bolometric correction and flux

Compiler	V	M_V	M_{bol}	BC_V	f x10^6 erg cm^{-2}s^{-1}	F x10^{10} erg cm^{-2}s^{-1}	L x10^{33} erg s^{-1}	Ref
	mag	mag	mag	mag				
BCP97	-26.76	4.81	4.74	-0.07	1.371	6.334	3.856	this paper
Allen	-26.74	4.83	4.75	-0.08	1.360	6.284	3.826	AQ 76
Durrant	-26.70	4.87	4.74	-0.13	1.370	6.329	3.853	LB VI/2a 81
Schmidt-Kaler	-26.74	4.83	4.64	-0.19	1.370	6.33	3.85	LB VI/2b 82
Lang*	-26.78	4.82	4.75	-0.07	1.372	6.34	3.86	AD 91

*The apparent V and apparent bolometric magnitude for the sun given by Lang are inconsistent with his absolute magnitudes (differs by 0.03 mag).

V magnitudes computed from the empirical solar spectrum and the model solar spectra (see Table A3).

Table A4 summarizes the solar parameters presented here and those from several well-known reference books for comparison.

Appendix E: concerning the theoretical realisations of standard system magnitudes and colors

The theoretical colors and magnitudes presented in this paper were computed using passband sensitivity functions claimed to represent those of the standard UBVRIJHKL system (Bessell 1990; Bessell & Brett 1988). These passbands were essentially reversed engineered, that is, commencing with a passband based on an author's prescription of detector and filter bandpass, synthetic colors were computed from absolute or relative absolute spectrophotometric fluxes for stars with known standard colors. By slightly modifying the starting passband (shifting the central wavelength or altering the blue or red cutoff) and recomputing the synthetic colors it is usually possible to devise a bandpass that generates magnitudes that differ from the standard magnitudes *within the errors* by only a constant that is independent of the color of the star. It is usually taken for granted that such a unique passband exists and that given a large enough set of precise spectrophotometric data and sufficient passband adjustment trials it can be recovered. However, there are several reasons why this may not be the case, at least not across the complete temperature range.

E.1. Standard systems may no longer represent a real system

Whilst the original system may have been based on a real set of filters and detectors, the original set of standard stars would almost certainly have been obtained with lower precision than is now possible and for stars of a restricted temperature and luminosity range. The filters may have also been replaced during the establishment of the system and the later data linearly transformed onto mean relations shown in the previous data. In addition, the contemporary lists of very high precision secondary standards that essentially define the "standard systems" have all been measured using more sensitive equipment with different wavelength responses. Again, rather than preserve the natural scale of the contemporary equipment the measurements have been "transformed" to some mean representation of the original system by applying one or more linear transformations or even non-linear transformations. To incorporate bluer or redder stars than those in the original standard lists, extrapolations have also been made and these may have been unavoidably skewed by the imprecision of the original data and the small number of stars with extreme colors in the original lists. As a result, the contemporary standard system, *although well defined observationally* by lists of stars with precise colors and magnitudes, *may not represent any real linear system* and is therefore impossible to realize with a unique passband. In fact, we should not be trying to find a unique passband with a central wavelength and shape that can reproduce the colors of a standard system but we should be trying to match the passbands and the linear or non-linear transformations used by the contemporary standard system authors such as Landolt, Cousins and Menzies et al. to transform their natural photometry onto the "standard system". That is why it is important for photometrists to publish the full details of their transformations and other details of their data reductions, such as extinction corrections.

E.2. Corrections between contemporary natural systems and thestandard UBVRI system

Menzies (1993) details the linear and non-linear transformations that have been used over the past 10 years to correct the SAAO natural system to the standard Cousins UBVRI system. Standard non-linear corrections are first made to the raw magnitude data in V, B-V, U-B, V-R and V-I. The resultant values are then linearly transformed to the standard system. In a further refinement, Kilkenny et al. (1997) detail systematic non-linear corrections that have been necessary to correct the V, B-V and V-I colors of the bluest and reddest stars.

Summarising the SAAO results, their current instrumental magnitudes require three sets of corrections, one for the O and B stars, another for the A to early K stars and another for the late K to late M stars. The maximum non-linear corrections are 0.06 to 0.10 mag for the reddest stars. The corrections for the bluest stars amount to less than 0.03 mag. After the non-linear corrections were made, the resultant linear relations were V= v + 0.012(b-v), B = b + 0.027(b-v), U = u -0.022(u-b) for blue stars and U = u - 0.005(u-b) for the red stars.

Landolt (1983, 1992) has not detailed as clearly the corrections made from his instrumental system to the standard system but he does give U-B = 0.925 (u-b) for the bluest stars and 1.026(u-b) for the remaining stars. As discussed by Bessell (1990), Landolt's B passband is bluer than the Johnson/Cousins natural B and Graham (1982) needed corrections of up to 0.10 (B-V) to correct his natural colors using similar filters. Small systematic differences between Landolt and Cousins VRI colors for the reddest stars resulted from Cousins use of two linear relations for his V-R and V-I transformations while Landolt used a single relation.

As the standard systems have been established from natural system colors using linear and non-linear corrections of at least a few percent, we should not be reluctant to consider similar corrections to synthetic photometry to achieve good agreement with the standard system across the whole temperature range of the models.

E.3. Corrections applied to the synthetic photometry

There are too few stars with accurate spectrophotometric fluxes and standard colors to be able to compare empirical synthetic colors with observed standard colors with a high degree of certainty for all spectral types and for all colors. We decided therefore to use synthetic colors computed from the models and compare them with the mean observed color-color relations and the mean color-temperature relations. In this way, even if the model colors are not perfect, we can use them to interpolate between stars of different gravity and different abundance with a high degree of confidence. Preliminary comparisons indicated that the computed model V, B-V, V-R and V-I colors relevant to A to K stars were in reasonable agreement with observations while the U-B comparison was much poorer

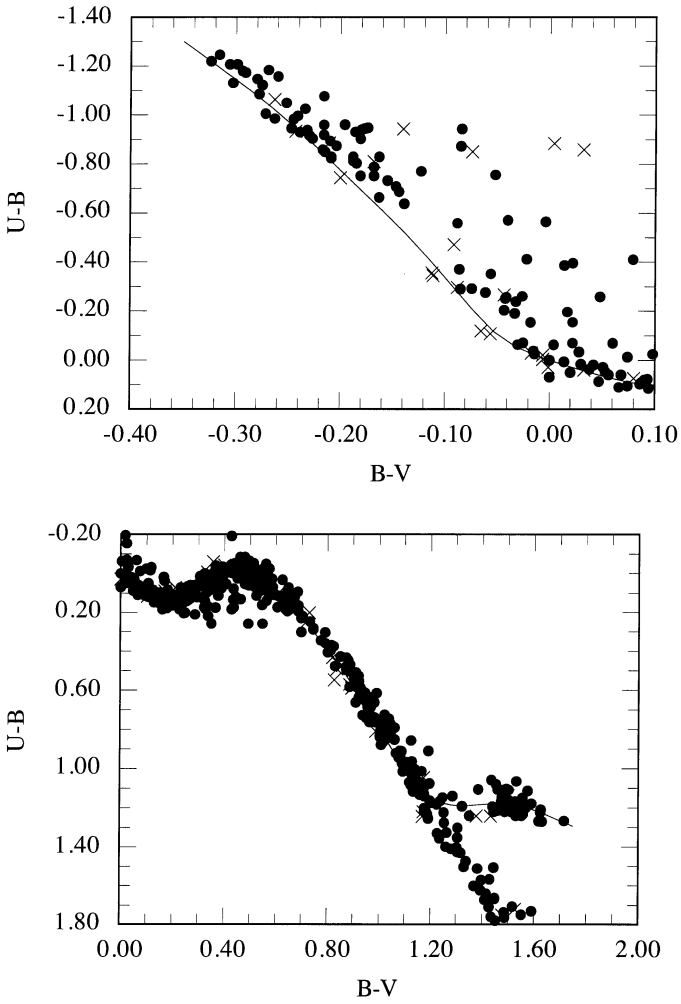

Fig. A1a and b. The observed U-B versus B-V diagram for the SAAO version of the UBV system; see text for references. The line represents a mean unreddened locus for dwarf stars.

E.3.1. The U-B color

That the U-B results were not as good as other colors should not have been too unexpected given the uncertainty in the U passband (Bessell 1986). Buser (1978) had devised a U passband by arbitrarily shifting the U3 passband of Azusienis and Straizys (1966); Bessell (1986, 1990) had attempted to reproduce the U response function by combining the transmission of the U filter glass, the response of a 1P21 phototube and included some atmospheric extinction. This passband matched the red cutoff of the Buser response but had a blue cutoff about 100 further to the UV. The Buser realisations of the UBV bandpasses had been used by Kurucz for the CDROM 13 colors.

The intrisic UBV colors for dwarf stars should be well established, but because of differences between versions of the standard system and uncertainties in the interstellar reddening for early type stars it is in fact not so clear. In Figs. A1a, b we plot the collected E-region photometry of Menzies et al (1980) and the selected bluest and reddest dwarf stars from Kilkenny et al. (1997): (solid circles), together with some older bright star photometry by Cousins of stars in common with Johnson (crosses). The smooth curve drawn in these figures is an attempt to represent the mean unreddened locus for dwarf stars so that we can use it in comparison with model colors. We note that this locus could perhaps have been drawn slightly bluer in B-V to make a greater allowance for reddening. In Figs. A2a, b we show such diagrams. The theoretical data (crosses) are plotted for log g=4.0 and 4.5 for $T_{eff} > 6000$K and for log g=4.5 and 5.0 for $T_{eff} < 5500$K.

To achieve the agreement in the range of the U-B colors between O and K stars shown in Figs A2a,b we have multiplied the U-B colors computed using the Bessell (1990) UBV passbands by 0.96. The resulting agreement is excellent except for the mid-A stars where the observed U-B colors appear slightly redder than the computed colors; however, there are several reasons why in this restricted color regime U-B colors in particular are uncertain. It is the temperature range where the hydrogen lines and the Balmer discontinuity are near their maximum strengths and the computed U and B magnitudes are correspondingly very sensitive to the exact positioning of the edges of the U and B passbands. There are also some uncertainties in the handling of the computation of the overlapping hydrogen lines near the

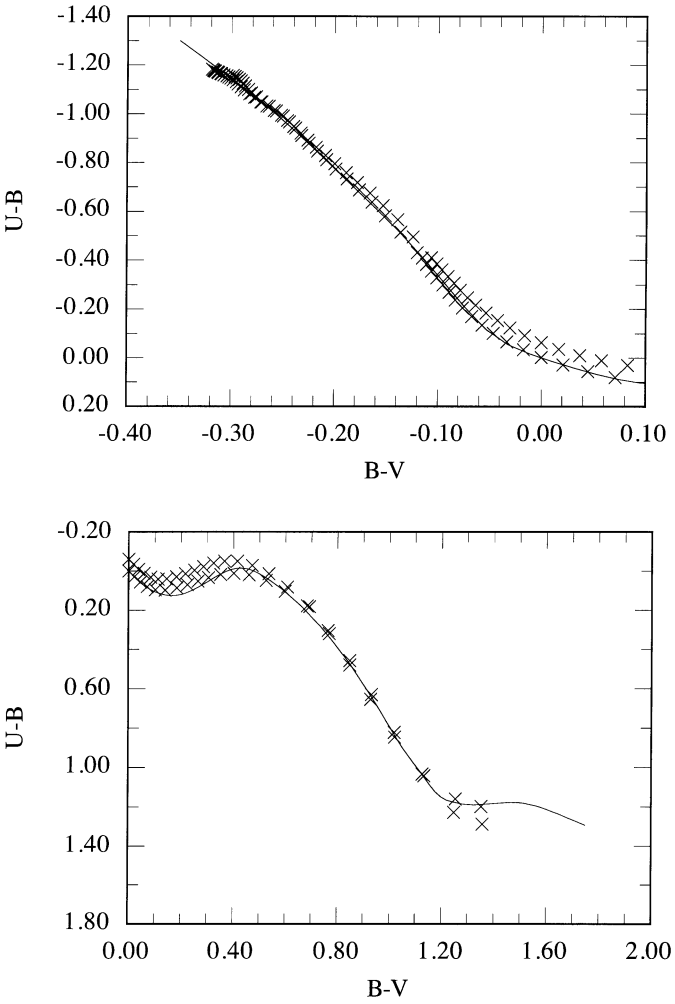

Fig. A2a and b. The theoretical U-B versus B-V digram is plotted for log g=4.0 and 4.5 for $T_{eff} > 6000$K and for log g=4.5 and 5.0 for $T_{eff} < 5500$K (crosses). It is compared with the observed unreddened dwarf locus.

Balmer series limit. It is also the color range where small non-linear corrections are often made in U-B transformations and where systematic differences in photometry result from how atmospheric extinction corrections are made, that is, how the discontinuity in the U or U-B extinction coefficient is handled (Cousins 1997). So we should not let a slight disagreement in the U-B colors of the A stars detract from the good agreement at other temperatures.

The U-B versus B-V comparison for colors computed using the Buser (1978) passbands are similar. They fit the B stars' relation well (except perhaps for the bluest stars) but diverge for the late-F to K star models. The differences for the reddest stars can be removed by scaling the U-B colors for those models redder than B-V=0.4 by 0.96. Given the uncertainties in the observed U-B versus B-V relation both sets of scaled colors can be said to fit the data, but overall, the scaled Bessell U-B colors produce slightly better agreement than the scaled Buser U-B colors.

The Landolt (1983) version of the U-B system differs systematically from the SAAO (Cousins) U-B system (see eg. Bessell 1995). The differences range from -0.10 mag for the bluest stars (Landolt values are bluer) to +0.05 for the reddest stars. A scale factor of 1.03 removes some of this difference but leaves systematic residuals with B-V (or U-B) color. These residuals exhibit the same shaped variation with color as seen in the differences Bessell - Buser but have higher amplitude. This suggests that the Landolt U-B system has a U band whose blue wing extends much further to the UV than does the SAAO U band. The unscaled U-B colors computed using the Bessell (1990) passbands represent the Landolt U-B versus B-V relation quite well although again the observed U-B colors of the mid-A stars are redder than the models.

Although for this paper we have decided to use the scaled U-B colors computed using the Bessell (1990) U passband, it would certainly be worthwhile to experiment more with other U passbands and the theoretical fluxes to try and better fit the observed U-B versus B-V relation.

E.3.2. Other colors

Slight adjustments to the B-V colors could be considered based on the U-B versus B-V diagram comparisons that indicate that the hottest models may need their B-V colors corrected by -0.01 or -0.02 mag, but given the uncertainties and the insensitivity of the B-V color to temperature we have made no changes. The slope change made by many observers in the B-V transformation for stars redder than B-V=1.5 suggests that we should perhaps also consider increasing the B-V colors of the redder models; we have not yet done so.

The theoretical V-R, R-I and V-I colors should probably also be adjusted for the M stars as most natural systems required two slopes for transformation onto the standard system. But we will await on better comparison data for the reddest stars before doing so.

E.4. Energy integration versus photon counting: observational and computational differences

There is another subtle reason why band-pass matching, linear transformations and synthetic photometry can be confusing in modern photometry. This is a result of a switch from flux measurements by energy integration across a wavelength band to photon integration across the same band. The resulting colors and magnitudes are not the same.

Most standard system photometry was carried using with photomultiplier tubes with current integration. This is equivalent to convolving the f_λ spectrum of a star in energy units by the bandpass sensitivity function. That is, the energy measured across a bandpass X is

$\int f(\lambda) R_X(\lambda) d\lambda$ where $R_X(\lambda)$ is the response function of the system.

If instead the number of detected photons across the passband X are counted, the number is:

$\int (f(\lambda)/h\nu)\, R_X(\lambda) d\lambda = \int (\lambda f(\lambda)/hc)\, R_X(\lambda) d\lambda$

Table A5. Color excess ratios to E(B-V) for E(B-V) = 0.29 - 0.024(B-V)

	E(U-B)	E(V-R)	E(R-I)	E(V-I)	E(V-K)	E(J-K)	E(H-K)	E(K-L)
B star	0.71	0.57	0.74	1.31	2.86	0.58	0.23	0.19
B-K star	0.71+	0.58+	0.74+	1.32+	2.91+	0.59+	0.23+	0.19+
color term	0.24(B-V)	0.09(V-R)	0.04(R-I)	0.06(V-I)	0.07(V-K)	0.06(J-K)	0.15(H-K)	0.17(K-L)

Table A6. Absorption ratios to A(V) for A(V) = 3.26 + 0.22(B-V)

	A(U)	A(B)	A(R)	A(I)	A(J)	A(H)	A(K)	A(L)
B-K star	1.32	1.09	0.82	0.59	0.29	0.23	0.11	0.05

This in essence weights the fluxes by the wavelength. The net effect is to shift the apparent effective wavelength of a passband for stars of different temperature more when photons are counted than when the energy is measured. The equi-energy effective wavelength will be different to the equi-photon effective wavelength indicating that a small linear transformation is required to the photon counting colors to match the energy derived colors. The effects are larger for broad bands and usually larger in the UV because the same width bandpass is a larger fraction of the wavelength for smaller wavelengths. CCDs and IR array detectors are all photon counting devices and this effect should be considered in comparisons between synthetic photometry and observations made with these devices.

Appendix F: effective wavelengths and reddening ratios

In broad-band photometry the nominal wavelength associated with a passband (the effective wavelength) shifts with the color of the star. For Vega the effective wavelength of the V band is 5448Å and for the sun it is 5502Å.

The effective wavelength of the V band (response function $R_V(\lambda)$ for an object with flux $f(\lambda)$ is

$$\lambda_{eff} = (\int \lambda\, f(\lambda)\, R_V(\lambda)\, d\lambda) / (\int f(\lambda)\, R_V(\lambda)\, d\lambda)$$

The effective wavelengths of the V band for different spectral types are B0: 5430Å, A0: 5450Å, F0: 5475Å, G2: 5502Å, K0: 5515Å, M0: 5597Å, M5: 5580Å. Some bands, such as the R band show much greater shifts (eg. Bessell 1986).

Interstellar reddening estimates are also affected by effective wavelength shifts which result in different values of reddening being derived from stars of different color. That is, a given amount of dust obscuration will produce a larger E(B-V) value for OB stars than for GK stars.

We have investigated quantitatively the effects of interstellar extinction on colors in the UBVRI system by multiplying model spectral fluxes with the extinction law summarised by Mathis (1990). Comparison between the synthetic photometry of the ATLAS9 models before and after application of an amount of interstellar extinction (corresponding to a nominal E(B-V)=0.30) gave us the color excess and magnitude ratios given in Tables A5 and A6. Note that the color excess ratios increase with color mainly as a result of E(B-V) decreasing with color.

The reddening ratios quoted in the literature are usually based on empirical reddening measurements using OB stars so would probably represent a mean $(B-V)_0$ of about -0.15 or an effective temperature around 15000K. The relevant theoretical ratios are shown in line 1 of Table A5. The values given in line 3 are color corrections to be added to the value in line 2 to account for changing color excess ratios with color. These derived relations show that when correcting for interstellar extinction a mean E(B-V) excess should not be applied to all stars but that the color excess should be scaled according to the intrinsic color of the star. The ratios to A(V) (Table A6) are less sensitive to the color. The good agreement between the calculated and observed ratios indicates that if the Mathis table is a good representation of the reddening then the passbands adopted for the UBVRIJHKL system are also a reasonable representation of the real passbands. The extinction law of Ardeberg & Virdefors (1982) although in agreement with the Mathis curve for BVRI produces a higher extinction in the U band that results in a calculated E(U-B)/E(B-V) ratio of 0.82 rather than 0.71 .

The reddening independent parameter Q is often used as a temperature index for OB stars. If we derive Q = (U-B) - 0.71(B-V) from our theoretical colors and regress against B-V, we find Q= 3(B-V). Therefore, we predict for OB dwarfs that E(B-V) = (B-V) - {(U-B) - 0.71(B-V)}/3.

References

Allard, F., Hauschildt, P.H. 1995, ApJ 445, 433

Allard, F., Hauschildt, P.H., Baraffe, I., Chabrier, G. 1996 ApJL 465, L123

Allard, F., Hauschildt, P.H., Miller, S., Tennyson, J. 1994, ApJL 426, L39

Allen, C.W. 1976, Astrophysical Quantities (The Athlone Press)

Allen, D.A., Tinney, C.T. 1981/97 www.aao.gov.au/local/www/cgt/irisguide

Aller, L.H. 1963, The Atomsphere of the Sun and Stars, N.Y. Ronald Press

Alvarez, R., Plez, B. 1997, A&A, in press

Ardeberg, A., Virdefors, B. 1982, A&A 115, 347

Alonso, A., Arribas, S., Marinez-Roger, C. 1996, A&AS 117, 227 (AAM96)

Azusienis, A., Straizys, V. 1966, Bull.Vil.Astr.Obs No 16, 3

Bell, R.A., Gustafsson, B. 1989, MNRAS 236, 653

Bertelli, G., Bressan, A., Chiosi, C., Lub, J. 1994, A&AS 106, 275

Bessell, M.S. 1979, PASP 91, 589

Bessell, M.S. 1986, PASP 98, 1303

Bessell, M.S. 1990a, PASP 102, 1181

Bessell, M.S. 1990b, A&AS 83, 357

Bessell, M.S. 1991, AJ 101, 662

Bessell, M.S. 1992, in "New Aspects of Magellanic Cloud Research", eds B. Baschek, G. Klare, J. Lequeux; Springer-Verlag Heidelberg, p321

Bessell, M.S. 1995, in "The Bottom of the Main Sequence - and Beyond", ed. C.G. Tinney, Springer-Verlag, Heidelberg, p129
Bessell, M.S., Brett, J.M. 1988, PASP 100, 1134
Bessell, M.S., Plez, B. 1997, in preparation
Bessell, M.S., Wood, P.R. 1984, PASP 96, 247
Bessell, M.S., Brett, J.M., Scholz, M., Wood, P.R. 1989, A&A 213, 209
Bessell, M.S., Brett, J.M., Scholz, M., Wood, P.R. 1991, A&AS 89, 335. Erratum 244, 251
Bessell, M.S., Scholz M., Wood, P.R. 1996, A&A 307, 481
Blackwell, D.E., Lynas-Gray, A.E. 1994, A&A 282, 899 (BLG94)
Blackwell, D.E., Leggett, S.K., Petford, A.D., Mountain, C.M., Selby, M.J. 1983, MNRAS 205, 897
Boeshaar, P.C. 1991, PhD. thesis, Ohio State Univ.
Böhm-Vitense, E. 1982, ApJ 255, 191
Brett, J.M. 1995 Private communication
Brett,J.M. 1995a, A&A 295, 736
Brett, J.M. 1995b, A&AS 109, 263
Brett, J.M. & Plez, B. 1993, PASAu 10, 250
Burnstein, D., Heiles, C. 1982, AJ 87, 1165
Buser, R. 1978, A&A 62, 411
Buser, R. and Kurucz R.L. 1978, A&A 70, 555
Caldwell, J.A.R., Cousins, A.W.J., Ahlers, C.C., van Wamelen, P., Maritz, E.J. 1993 SAAO Circ 15, 1
Carter, B.S. 1990, MNRAS 242, 1
Castelli, F. 1995-97, private communication
Castelli, F. 1996 Proceedings of the Workshop on Model Atmospheres and Spectrum Synthesis, ASP Conference Series 108, ed. S. Adelman, F. Kupka & W. Weiss, p.108
Castelli, F., Kurucz, R. L. 1994, A&A 281, 817
Castelli, F., Gratton, R.G., Kurucz, R.L. 1997, A&A 318, 841
Cayrel de Strobel, G. 1996, A&ARv 7, 243
Cayrel, R. 1997, private communication
Chabrier, G., Baraffe, I. 1995, ApJL 451, L29
Chabrier, G., Baraffe, I., Plez, B. 1996, ApJL 459, L91
Charbonnel, C., Meynet, G., Maeder, A., Schaller, G., Schaerer, D. 1993, A&AS 101, 415
Code, A.M., Davis, J., Bless, R.C., Hanbury Brown ,R. 1976, ApJ 203, 417
Colina, L., Bohlin, R.C., Castelli, F. 1996, AJ 112, 307
Cohen, M., Walker, R.G., barlow, M.J., Deacon, J.R. 1992, AJ 104, 1650
Cousins, A.W. 1972, MNASSA 31, 69
Cousins, A.W. 1976, MemRAS 81, 25
Cousins, A.W. 1980a, SAAO Circ 1, 166
Cousins, A.W. 1980b, SAAO Circ 1, 234
Cousins, A.W. 1980c, SAAO Circ 6, 4
Cousins, A.W. 1987, SAAO Circ 11, 93
Cousins, A.W. 1997, preprint
Crowther, P.A. 1997, in Fundamental Stellar Properties, IAU Symposium 189, eds. T.R. Bedding, A.J. Booth, J. Davis, in press
Duncan, C.H., Willson, R.C., Kendall, J.M., Harrison, R.G., Hickey, J.R. 1982, Sol.En. 28, 385
Durrant, C.J. 1981, Landolt Börnstein vol VI/2A (Neue Series: Springer-Verlag), p82
Di Benedetto, G.P., Rabbia, Y. 1987, A&A 188, 114
Doverstål, M., Weijnitz, P. 1992, Mol. Phys. 75, 1375
Dreiling, L.A., Bell, R.A. 1980, ApJ .241, 736
Dyck, H.M., Benson, J.A., van Belle, G.T., Ridgway, S.T. 1996, AJ 111, 1705
Fitzgerald, M.P. 1968, AJ 73, 983
Frogel J.A., Persson S.E., Cohen T.G. 1981, ApJ 246, 842
Furenlid, I., Westin, T., Kurucz, R.L. 1995, Laboratory and Astronomical High Resolution Spectra, ASP Conf. Series, Vol. 81, 1995, p.615
Glass, I. 1997 Private communication
Graham, J. 1982, PASP 94, 244
Gustafsson B., Bell R.A. 1979, A&A 74, 313
Gustafsson B., Bell R.A., Eriksson K., Nordlund Å. 1975, A&A 42, 407
Habets G.M.H.J., Heintze J.R.W. 1981, A&AS 46, 193
Hardorp, J. 1980, A&A 91, 221
Hauck, B., Mermilliod, M. 1990, A&AS 86, 107
Hayes, D.S. 1985, in IAU Symposium 111, "Calibration of Fundamental Stellar Quantities", Eds. D.S. Hayes et al. (Reidel: Dordrecht), p.225
Hedgecock, I.M., Naulin, C., Costes, M. 1995, A&A 304, 667
Höfner, S., Dorfi, E.A. 1997, A&A 319, 648
Johnson, H. 1966 ComLPL 4, 99
Jørgensen U.G. 1996, private communication
Karlsson, L., Lindgren, B., Lundevall, C., Sassenberg, U. 1997, J. Mol. Spec. 181, 274
Kilkenny et al. 1997, preprint
Kurucz, R.L. 1979, ApJS 40, 1
Kurucz, R.L. 1989, private communication
Kurucz, R.L. 1991, Stellar Atmospheres: Beyond Classical Models, eds. Crivellari et al., Kluwer Academic Publisher, p.441
Kurucz, R.L. 1992, Stellar Popuation of Galaxies, IAU Symp. 149, ed. Barbuy B. & Renzini A., p.225
Kurucz R. L. 1993, CD-ROM No 13
Kurucz R. L. 1994, CD-ROM No 19
Kurucz R.L 1995 a, private communication
Kurucz R.L 1995 b, CD-ROM No 23
Lacy C.H. 1977, ApJ 218, 444
Landolt, A.U. 1983, AJ 88, 439
Landolt, A.U. 1992, AJ 104, 340
Lang, K.R. 1991 Astrophysical Data: Planets and Stars (Springer-Verlag), p103
Langhoff, S.R. 1997, ApJ 481, 1007
Leggett, S.K., Bartholomew, M., Mountain, C.M., Selby, M.J. 1986, MNRAS 223, 443
Leung K-C., Schneider D. 1978, AJ 83, 618
Mathis, J. 1990 A.R.A&A. 28, 37
Menzies, J.W. 1993 in Precision Photometry: Eds. D. Kilkenny, E. Lastovica, J.W. Menzies, SAAO, p35.
Menzies, J.W., Banfield, R.M., Laing, J.D. 1980, SAAO Circ. 5, 149
Megessier C. 1994, A&A 289, 202
Megessier C. 1995, A&A 296, 771
Morton, D.C., Adams, T.F. 1968, ApJ 151, 611
Mountain, C.M., Selby, M.J., Leggett, S.K., Blackwell, D.E., Petford, A.D. 1985, A&A 151, 399
Neckel, H., Labs, D. 1984, Sol.Phys.,90, 205
Partridge, H., Schwenke, D.W. 1997, J. Chem. Phys. 106, 4618
Perrin, G., Coude du Foresto, V., Ridgway, S.T., Mariotti, J.-M., Traub, W.A., Carleton, N.P., Lacasse, M.G. 1997, A&A , in press
Piskunov, N.E., Kupka F., Ryabchikova T.A., Weiss W.W., Jeffery C.S. 1995, AAS 112, 525.
Plez, B. 1992, A&AS 94, 527
Plez, B. 1995-7 Private communication
Plez, B., Brett J.M., Nordlund Å. 1992, A&A 256, 551
Plez B., Edvardsson B., Gustafsson B., Eriksson K., Jorgensen, U.G. 1997, in preparation

Reid, I.N., Gilmore, G.F. 1984, MNRAS 206, 19
Ridgway, S.T., Joyce, R.R., White, N.M., Wing, R.F. 1980, ApJ 235, 126
Schaerer, D., Charbonnel, C., Meynet, G., Maeder, A., Schaller, G. 1993b, A&AS 102, 339
Schaerer, D., Meynet, G., Maeder, A., Schaller, G. 1993a, A&AS 98, 523
Schaller, G., Schaerer, D., Meynet, G., Maeder, A. 1992, A&AS 96, 269
Schmidt-Kaler, Th. 1982, in: Landolt-Börnstein, Numerical Data and Functional Relationships in Science and Technology, Vol. 2. (eds.) K. Schaifers & H.H. Voigt Springer-Verlag, Berlin, p.451
Scholz, M., Takeda, Y. 1987, A&A 186, 200 (erratum: 196, 342)
Selby, M.J., Mountain, C.M., Blackwell, D.E., Petford, A.D., Leggett, S.K. 1983, MNRAS 203, 795
Stebbins, J., Kron, G.E. 1957, ApJ 126, 226
Sung, H. 1997, private communication
Taylor, B.J. 1992, PASP 104, 500
Tinney, C.G., Mould, J.R., Reid, I.N. 1993, AJ 105, 1045
Tsuji, T. 1981a JApA 2, 95
Tsuji, T. 1981b A&A 99, 48
Tsuji, T., Ohnaka, K. 1995, in Elementary Processes in Dense Plasmas, eds. S. Ichimaru and S. Ogata, Addison-Wesley, p.193
Tsuji, T., Ohnaka, K., Aoki, W. 1995, in The Bottom of the Main Sequence and Beyond, ed. C.G. Tinney, Springer, p. 45
Tsuji, T., Ohnaka, K., Aoki, W. 1996a, A&A 305, L1
Tsuji, T., Ohnaka, K., Aoki, W., Nakajima, T. 1996b, A&A 308, L29
Wood, P.R., Bessell, M.S. 1994, private communication by anonymous ftp